Contract No.:

This manuscript has been authored by Savannah River Nuclear Solutions (SRNS), LLC under Contract No. DE-AC09-08SR22470 with the U.S. Department of Energy (DOE) Office of Environmental Management (EM).

Disclaimer:

The United States Government retains and the publisher, by accepting this article for publication, acknowledges that the United States Government retains a non-exclusive, paid-up, irrevocable, worldwide license to publish or reproduce the published form of this work, or allow others to do so, for United States Government purposes.

Development and testing of a PEM SO_2-depolarized electrolyzer and an operating method that prevents sulfur accumulation

John L. Steimke[a,b,*], Timothy J. Steeper[a,c], Hector R. Cólon-Mercado[a], and Maximilian B. Gorensek[a]

[a]*Savannah River National Laboratory, Aiken, SC 29808 USA*
[b]*Current address: 1829 Robinson Drive, North Augusta, SC 29841 USA*
[c]*Current address: 725 Dayton Valley Road, Dayton, NV 89403 USA*

Abstract

The hybrid sulfur (HyS) cycle is being developed as a technology to generate hydrogen by splitting water, using heat and electrical power from a nuclear or solar power plant. A key component is the SO_2-depolarized electrolysis (SDE) cell, which reacts SO_2 and water to form hydrogen and sulfuric acid. SDE could also be used in once-through operation to consume SO_2 and generate hydrogen and sulfuric acid for sale. A proton exchange membrane (PEM) SDE cell based on a PEM fuel cell design was fabricated and tested. Measured cell potential as a function of anolyte pressure and flow rate, sulfuric acid concentration, and cell temperature are presented for this cell. Sulfur accumulation was observed inside the cell, which could have been a serious impediment to further development. A method to prevent sulfur formation was subsequently developed. This was made possible by a testing facility that allowed unattended operation for extended periods.

Keywords: electrolysis, hybrid sulfur cycle, SO_2-depolarized electrolysis, sulfuric acid

[*] Corresponding author. Tel.: (803) 442-9944; E-mail address: johnsteimke@comcast.net

Acronyms

ASR	Area specific resistance
BPR	Back pressure regulator
DOE	US Department of Energy
HTE	High-temperature electrolysis
HyS	Hybrid sulfur
INL	Idaho National Laboratory
MEA	Membrane electrode assembly
PBI	Polybenzimidazole
PEM	Proton exchange membrane (a.k.a. polymer electrolyte membrane)
PFA	Perfluoroalkoxy
PPS	Polyphenylene sulfide
PTFE	Polytetrafluoroethylene
SDE	SO_2-depolarized electrolyzer
SEM	Scanning electron microscopy
SRNL	Savannah River National Laboratory

1. Introduction

1.1. Background

Concerns about the potential for climate change due to anthropogenic CO_2 emissions from the combustion of fossil fuels along with the desire for a sustainable source of energy inevitably lead to hydrogen produced from renewable or nuclear sources as a possible alternative for future energy systems. Utilization of hydrogen in fuel cells is non-polluting and efficient.

Renewable sources are inexhaustible and clean. Properly managed, nuclear energy sources are virtually inexhaustible, with smaller footprints and potentially smaller life cycle impacts.

As a result, thermochemical cycles that can generate hydrogen by splitting water using high temperature heat from nuclear or concentrated solar sources have been the focus of considerable research efforts since they were first proposed in the 1960s [1]. One of these is the hybrid sulfur (HyS) cycle (also known as the Westinghouse cycle), which consists of a low temperature (~100ºC) and a high temperature (~1000ºC) step [2]. In the high temperature step, sulfuric acid is decomposed endothermically to SO_2, water, and oxygen co-product. In the low temperature step, after the oxygen is separated and removed, the remaining water and SO_2 are reacted electrochemically in SO_2-depolarized electrolysis (SDE) cells to form sulfuric acid and hydrogen product. SO_2-depolarization greatly reduces the cell potential needed to generate hydrogen as compared to conventional water electrolysis. Reversible and practical cell voltages for SDE are ~0.2 and ~0.7 V, respectively, whereas for conventional proton exchange membrane (PEM) water electrolysis, they are 1.23 and ~1.75 V, respectively. Sulfuric acid from the SDE cells is recycled back to the decomposer to close the cycle. (Alternately, SDE may be used with a source of SO_2 such as a smelter or coal fired power plant to generate sulfuric acid and hydrogen products.) Thermochemical water-splitting cycles offer the possibility of higher conversion efficiencies (with respect to the primary heat source) than direct water electrolysis because they can use heat directly without power conversion losses to drive one or more of the reaction steps (e.g., high temperature sulfuric acid decomposition in the case of HyS.

HyS is one of the simplest thermochemical water-splitting cycles, comprising only two reaction steps, having all fluid reactants and products, and with sulfur (cycling between its +4 and +6 oxidation states) the only other element required besides hydrogen and oxygen.

Consequently, its separation tasks are relatively simple, minimizing their potential impact on the net thermal efficiency for hydrogen production.

1.2. Previous work

Researchers at Westinghouse Electric Corporation, where HyS was first conceived [3], performed extensive early testing of SDE for hydrogen production during the period 1975-1983 [4-10]. Westinghouse tests used conventional parallel plate electrochemical cells. The anolyte was a sulfuric acid solution containing dissolved SO_2 flowing through a gap between the anode and a porous rubber membrane. The catholyte was a sulfuric acid solution, and similarly flowed between the cathode and the membrane.

After 1983, when the drive toward alternative energy sources dwindled with the global stabilization of petroleum supplies and prices, there was a period of inactivity for SDE development until 2003, when interest in a hydrogen economy began to grow once again. Savannah River National Laboratory (SRNL) received U. S. Department of Energy (DOE) funding to develop SDE for HyS under the Nuclear Hydrogen Initiative and issued a number of reports on electrolyzer development. Cólon-Mercado and Hobbs [11] evaluated a variety of potential catalysts for use with SDE. Elvington, et al. [12] tested a range of PEM materials such as Nafion®, PBI (polybenzimidazole), and polyphenylenes for properties such as chemical stability, durability, proton conductivity, and SO_2 flux. Cólon-Mercado, et al. [13] summarized the body of work related to SDE at SRNL up to that point.

Larger scale tests (54.8 cm^2 active cell area) at SRNL were reported by Steimke and co-workers [14-16] in which temperature, acid concentration and SO_2 concentration were varied. For the larger scale tests, SRNL developed an SDE cell and associated hardware patterned after conventional PEM fuel cells, albeit with liquid feeds streams. The intent of this approach was to

leverage ongoing developments in PEM fuel cell technology, which would ultimately lead to better and more economical SDE cell designs.

SRNL tested the performance and the effect of operating conditions for both short and long term operation of the cell. During the course of these tests, deposition of sulfur at the interface between the membrane and the cathode was observed, which could have made the liquid-fed PEM SDE approach impractical. Further testing and analysis resulted in the identification of an operating envelope that prevented the formation of such a sulfur rich layer. The discovery of this operating envelope was a major achievement and resulted in the granting of a US patent [17].

Water transport through a membrane electrode assembly (MEA) that operated with a gaseous SO_2 feed to the anode and water feed to the cathode was modeled by Staser and Weidner [18]. Staser et al. [19] quantified individual contributions to the total voltage drop. In particular, they examined water transport and diffusion of SO_2.

Stone et al. [20] tested an electrolyzer stack in which SO_2 was introduced in the gas phase and a low permeability pre-layer was used to reduce crossover of SO_2.

Jayakumar et al. [21] tested the use of PBI and Nafion® membranes in PEM SDE. Proton transport in PBI is less dependent on the water concentration in the membrane than in Nafion®. Therefore, PBI membranes are not as severely affected by operation at higher acid concentrations. Nafion® membrane dehydration is detrimental as it results in increased cell voltage. More concentrated sulfuric acid is clearly desirable for commercial applications. For tests using PBI membranes, water vapor and gaseous SO_2 were fed to the anode where they reacted to form sulfuric acid, and the cathode was kept dry. For tests with Nafion®, however, liquid water was fed to the cathode and anhydrous SO_2 was fed to the anode. Water diffused

across the membrane from the cathode to the anode, driven by the activity difference, where it reacted with SO_2 to make sulfuric acid. This kept the membrane hydrated. One characteristic of feeding gaseous SO_2 was that the concentration of the sulfuric acid product depended on the cell current. When using Nafion® membranes, increasing the acid concentration increased the area specific resistance (ASR) of the cell, which was expected. The effect was much smaller, however, with PBI membranes.

Kriek et al. [22] published a review paper on open cycle SDE for sulfuric acid and hydrogen production. Xue et al. [23] performed a thorough sensitivity study of differences in MEA preparation and SDE operating conditions. In all tests the MEA was constructed using a Nafion® 115 membrane. In MEA testing they varied weight percent acid in the anolyte, temperature and current. As expected, increases in each parameter increased cell voltage. They also varied Pt loading in the catalyst. Additional Pt loading decreased cell voltage up to a point. They developed an empirical correlation for cell voltage. Peach et al. [24] tested PBI and Nafion® membranes in an SDE cell. Dry SO_2 was fed to the anode and water was fed to the cathode. The product was 80% sulfuric acid solution. At low current densities the PBI membrane gave lower cell voltages than the Nafion® membranes. At higher current densities, the voltages were comparable. Allen et al. [25] studied the mechanisms of SO_2 oxidation in SDE using solid disk electrodes. They found that the oxidation is an oscillating reaction, that dithionate may be an intermediate, and that there is evidence for the formation of sulfur rich solids. Xue et al. [26] tested a range of bimetallic catalysts for SO_2 oxidation. Their goal was to find a cheaper substitute for the baseline catalyst, platinum. Platinum chromium bimetallic catalyst (60 wt% Pt) gave the best results. Cell performance degradation was attributed to the formation of sulfur rich solids.

1.3.Electrochemical reactions

The cell of the electrolyzer has two electrodes: an anode and a cathode. Electrical current passes through the cell which drives the following two reactions.

Anode: $SO_2(aq) + 2H_2O(l) \rightarrow H_2SO_4(aq) + 2H^+ + 2e^-, \quad E° = -0.158\,V$ (1)

Cathode: $2H^+ + 2e^- \rightarrow H_2(g), \quad E° = 0.0\,V$ (2)

Protons (hydronium ions) move from the anode to the cathode through the PEM, while electrons flow from the anode to the cathode through an external circuit, recombining to form molecular hydrogen. The net reaction is shown in (3).

Net reaction: $SO_2(aq) + 2H_2O(l) \rightarrow H_2SO_4(aq) + H_2(g), \quad E° = -0.158\,V$ (3)

The standard cell potential for this reaction is -0.158 V [27]. This assumes all reactants and products are at their standard states. The reversible cell potential at the actual conditions in the electrolyzer, E_{rev} may be calculated from this value using the well-known Nernst equation. The actual operating voltage, E_{oper} contains additional contributions, as shown in (4),

$$E_{oper} = E_{rev} + \eta_a + \eta_c + \eta_{ohm} + \eta_{hw} \quad (4)$$

where E_{rev} is the reversible cell potential or potential at very low current, which is a weak function of temperature and a stronger function of acid concentration;

η_a is the anode overpotential, which is a function of the effective surface area of the catalyst, catalyst type, current density, SO_2 concentration, and acid concentration;

η_c is the cathode overpotential, which is smaller than the anode overpotential and is a function of catalyst surface area, catalyst type and current density;

η_{ohm} is the ohmic loss, which is due to the resistance across the fluids and the membrane and is proportional to current density; and

η_{hw} is the hardware loss, which is proportional to current density.

A more detailed explanation and quantification is provided in [19].

2. Experimental

2.1. Description of the electrolysis cell

The SRNL electrolysis cell is of the PEM MEA type. The MEA is a "sandwich" consisting of an electrically conducting flowfield, an anode where anolyte (an aqueous solution of SO_2 and sulfuric acid) is oxidized to produce hydrogen ions and sulfuric acid, an electrically insulating PEM that allows hydrogen ions and water to pass through, a cathode where the hydrogen ions are reduced to hydrogen gas, and another electrically conducting flowfield. The remainder of the electrolyzer serves to deliver fresh anolyte containing the reactants to the anode and to remove spent anolyte containing the sulfuric acid reaction product, to remove wet hydrogen gas and any by-products from the cathode, to provide current paths to the electrodes, to allow temperature control, and to contain the internal pressure.

Photographs of the SRNL electrolysis cell are provided in **Figure 1**. Proceeding from the anode side of the cell to the cathode side, the following layers can be found, with thicknesses noted: stainless steel heated pressure plate (25.4 mm), Kynar® insulator (0.3 mm), copper terminal plate (3.4 mm), non-porous graphite seal block (12.7 mm), inter-digitated graphite flowfield with ten narrow channels (2.5 mm), non-PTFE (polytetrafluoroethylene) coated carbon paper (0.3 mm), Nafion® membrane with platinized carbon coated on both sides (0.3 mm), carbon cloth (0.15 mm), inter-digitated graphite flowfield with 30 channels (2.5 mm), another seal block (12.7 mm), another copper terminal plate (3.4 mm), fiberglass insulator (0.7 mm), and another stainless steel heated pressure plate (25.4 mm). Inter-digitated means that the inlet and outlet ports are connected to different finger-like channels cut into the flowfield, and that the

inlet and outlet channels are interspersed but do not connect directly. The carbon paper and cloth used in the cell were obtained from ElectroChem, Inc.

The pressure plates are 152 mm square and have twelve holes for Belleville spring washers and bolts torqued to 22 N-m that compress the cell to prevent leakage and maintain electrical continuity. The edge of both pressure plates has a deep hole for the insertion of a small cartridge heater. The face of the anode pressure plate also has two holes containing Teflon® inserts that are sealed to the pressure plate with Viton® O-rings. PFA (perfluoroalkoxy) tubes for anolyte to enter and exit the cell pass through holes and other Viton® O-rings in the Teflon® inserts. The Teflon® inserts also pass through a hole in the anode copper terminal plate where there is another Viton® O-ring. The copper terminal plates have large tabs to which heavy power cables are bolted. The anode copper terminal is pressed against the graphite seal block (120 mm square). One edge of each graphite seal block has two 50-mm deep, 1.6-mm diameter holes for PFA coated thermocouples to measure anode and cathode temperatures. An adjacent edge of each seal block has an attachment for a voltage tap. Anolyte flows through a hole in the seal block and to the graphite flowfield that sits in a recess machined into the seal block. The anode flowfield has ten channels that are 1.3 mm deep, 0.7 mm wide and 72 mm long, half connected to the anolyte inlet and half to the outlet. The geometry forces anolyte to flow from inlet channels, parallel to the face of the flowfield, through the electrically conducting porous carbon paper and also parallel to the platinized carbon layer forming the anode of the MEA. Anolyte is collected by the outlet channels. The cathode side of the MEA faces electrically conducting carbon cloth and a graphite flowfield with thirty channels. Half of the channels are connected to a water inlet and half are connected to the hydrogen (with a little water) outlet. The maximum active area of the cell is equal to 54.8 cm^2.

Design, fabrication, and operation of the SRNL cell represented a significant technical achievement. It was the first SDE cell based on a PEM fuel cell design, and its robust construction allowed for numerous tests over several years with a variety of MEAs. The maximum cell potentials encountered in SDE experiments were low enough to allow the use of graphite anodes instead of the titanium anodes typically found in PEM water electrolyzers, making the SRNL SDE cell much more like a PEM fuel cell operated "in reverse" as an electrolyzer. The intent was to facilitate leveraging future improvements in PEM fuel cell design.

2.2. Description and fabrication of the MEA

The SDE MEA uses a membrane with thin electrodes coated on both sides. The membrane, typically Nafion® 115, was coated with platinized carbon ink using a spray gun driven with argon carrier gas, as described previously (e.g., Elvington, et al. [12]). Platinum black, which has less surface area, was used for a few MEAs but resulted in higher cell voltages. The target metal loadings were typically 1.8 mg Pt/cm^2 and 0.8 mg Pt/cm^2 for the anode and cathode sides, respectively. The ink contained platinized carbon, water, methanol, and Nafion® dispersion. After spraying and drying the membrane, the MEA was hot pressed as a sandwich between sheets of Teflon® cloth and metal plates at 140ºC and 1.5 MPa for three minutes.

2.3. Balance of the electrolyzer facility

The electrolyzer facility is divided into two sections, the anolyte section and the hydrogen section, which are on the left and right hand sides of **Figure 2**, respectively. The anode chemical reaction, equation (1), consumes water and SO_2, both of which are supplied to the anolyte tank using accurate digitally controlled syringe pumps, Teledyne ISCO Model 500D. It was important to meter SO_2 to the absorber section of the anolyte tank in the liquid phase, not in the

gas phase, for accurate measurement. Three steps were taken to ensure SO_2 remained in the liquid phase. First, liquid phase SO_2 was drawn from the bottom of an inverted cylinder. Second, the SO_2 cylinder was heated to 40ºC with a blanket heater prior to transfer to increase its internal pressure and facilitate transfer to the syringe pump. Third, the SO_2 backpressure regulator (BPR) just downstream of the syringe pump was set above the vapor pressure of SO_2 at ambient temperature, which is 330 kPa(abs). The BPR prevented premature flashing and maintained the SO_2 loaded to the syringe in liquid form. When the control computer sensed a low inventory of SO_2 in the pump it changed the positions of valves and reversed direction of the syringe to refill from the supply cylinder. So, during the brief refilling period, no SO_2 was fed to the packed bed absorber.

The water syringe pump was refilled with deionized water from a pressurized header for quick and easy replenishment. Computer control metered the two reactants into the anolyte tank. Water was added at a controlled rate to maintain anolyte density, which is strongly dependent on acid concentration. If water had not been added, consumption of water and generation of sulfuric acid would have increased the sulfuric acid concentration with a corresponding increase in anolyte density. SO_2 was added at a controlled rate to maintain anolyte pressure. If SO_2 had not been added, consumption of SO_2 would have decreased the anolyte pressure and also the SO_2 concentration in the anolyte.

Initially, the anolyte pump was a magnetic drive gear pump with polyphenylene sulfide (PPS) gears and Carpenter Alloy 20 body. After hundreds of hours of operation, the body showed significant corrosion. Later, a small piston pump with Teflon® body and ceramic piston was successfully used. Feedback control utilizing the flow measurement at the magnetic flowmeter was used to control the anolyte flowrate at the specified setpoint. The commercial

flowmeter had zirconium electrodes and custom flanges with zirconium inserts which never suffered observable corrosion.

Fresh anolyte entered the anode side of the electrolyzer and exited enriched in sulfuric acid and depleted in SO_2 and water. Single pass conversion of SO_2 was typically 33%. Spent anolyte then flowed through an Anton Paar Type DTR 427 density meter with tantalum wetted surfaces for corrosion resistance.

Spent anolyte next passed into the top of the 1.2-m tall anolyte tank, which had two sections. The top section was a packed bed absorber filled with glass Raschig rings that were supported on a glass screen located 300 mm above tank bottom. The absorber allowed SO_2 gas to be absorbed into the anolyte. The bottom section was the anolyte reservoir. The ends of the anolyte tank were machined from Teflon® and were sealed with Viton® O-rings. The walls of the tank were three nested tubes. The inner and middle tubes were made from heavy wall borosilicate glass for corrosion resistance and clarity. The outer tube was made from clear acrylic for resistance to breakage. Hot water was pumped upward between the inner and middle tubes to heat the anolyte. The space between the middle and outer tubes trapped an air layer to decrease heat loss. Hot water was provided by a hot water bath that included a pump.

Because water and SO_2 were being added to the anolyte tank, anolyte volume slowly increased, so hardware was added to automatically control the anolyte inventory. Four laser beams positioned at different elevations below the Raschig rings were aimed across the anolyte tank, but off-center. Four light detectors were arranged on the opposite side of the tank at the same elevations, one per laser. When liquid anolyte was present the laser beam diffracted into its detector, otherwise it did not. Moving up from the bottom of the anolyte tank the elevations were low alarm (70 mm), low operating (120 mm), high operating (180 mm) and high alarm

(230 mm). When the high operating sensor detected liquid, the computer opened a motorized drain valve. When the low operating sensor stopped detecting liquid, the computer closed the valve. Discharged anolyte was collected in a drum. Occasionally a mechanical malfunction caused the anolyte level to go outside its normal range and register low alarm or high alarm. Then a repair was made.

The other side of the facility was the hydrogen handling side. A small flow of water, manually adjusted to about 10 mL/min, was fed to the cathode side to maintain good hydration of the membrane. Some of this water crossed the membrane to the anolyte because the activity of water at the cathode (essentially pure water) was greater than in the anolyte (sulfuric acid) and because the cathode pressure was usually maintained 33 kPa higher than the anode pressure. This provided a small water flux to counter the concentration driven flux of SO_2 from the anode side to the cathode side. It also provided some of the reaction water required at the anode. Water, hydrogen and a small concentration of hydrogen sulfide flowed out of the cell to a water/hydrogen separator, which had an infrared level detector. When the water level was higher than the infrared source and the detector, water absorbed the beam. The disrupted beam briefly opened the valve at the bottom of the separator. Water with some dissolved hydrogen sulfide flowed to a collection drum until the beam was reestablished and the valve closed.

Downstream of the separator was a BPR that maintained the pressure of the hydrogen and maintain a constant pressure difference across the membrane. Hydrogen flowed from the BPR to a gas flowmeter calibrated for hydrogen. Part of the gas flow passed through a gas chromatograph to measure hydrogen sulfide concentration.

2.4.Materials observations

Initially, some components used in the hydrogen product stream were constructed from Type 316 stainless steel and showed no corrosion. After the method of operation was changed to prevent sulfur layer formation, an unexpected result was that the hydrogen stream became corrosive to the stainless steel, whereas it had not been before. Apparently the altered composition of the product stream de-passivated stainless steel. Stainless steel components before the water separator were subsequently replaced with PFA or Teflon® components, which solved the problem. Downstream of the water separator, where almost all of the water was removed, the hydrogen stream was not corrosive to stainless steel.

Titanium components were used briefly but were quickly corroded by hot anolyte. Zirconium and tantalum were both resistant to hot anolyte. The seal blocks of the cell were machined from graphite. Both porous and non-porous graphite are available for sale. It was learned that the seal blocks must be made from non-porous graphite to prevent slow leaks.

3. Experimental

3.1.Observations of cell voltage increase and sulfur formation

A total of 37 MEAs was tested with the SDE cell. **Table 1** summarizes the characteristics of the MEAs that were tested. Results for a few of these tests are presented here.

During early testing of MEAs at SRNL, it was observed that cell voltage generally increased over the period of testing for an MEA, which was usually intermittent and conducted only during daytime hours over a period as long as two months. At the time, it was not known whether the increase in voltage was the result of membrane degradation, catalyst poisoning, or some other cause. This observation was complicated by the fact that cell voltage is influenced

by current density, cell temperature, anolyte pressure (which affects concentration of SO_2 in the anolyte), anolyte flowrate, membrane material and thickness, catalyst loading, and concentration of sulfuric acid in the anolyte. The first longevity test, which used MEA 12, provided valuable information about the process of cell voltage increase because it was run for 100 continuous hours at nearly constant conditions.

MEA 12 was tested briefly on a Friday at ambient conditions and cell voltages were among the lowest for ambient conditions that had been measured up to that time. Over the weekend the cell was stored with the anode immersed in anolyte saturated in SO_2 and the cathode was exposed to hydrogen gas. The test resumed the following Monday morning. The cell voltage for ambient conditions and the same current as Friday was 90 mV higher. Temperature and pressure were then increased to 80°C and 4 bar and held there for 100 continuous hours. Both of those increases decreased cell voltage, as expected. Anode and cathode pressures were held equal. Anolyte flowrate was 80 mL/min and anolyte acid concentration was 30 wt%. Catholyte flush water flowrate was 2 mL/min. For a constant current density of 365 mA/cm^2 (20 A) the voltage gradually increased from 0.78 V to 0.84 V over 100 hours. In addition, the pressure drop for constant flow of anolyte through the cell increased from 10 kPa to 27 kPa.

An additional observation was made during this 100-hr test. During initial ambient condition startup on the first day of continuous testing, colloidal sulfur was observed in the water/hydrogen separator, but no additional sulfur was observed there after a couple of hours into the run. At the end of the test, MEA 12 was cleaned and mounted for scanning electron microscopy (SEM). As show in **Figure 3**, a thick sulfur rich layer was found between the cathode and membrane. This layer registered 58.7% sulfur and for this situation had the same

thickness as the membrane. The anode, cathode and membrane were expected to register some sulfur because sulfur is a constituent of Nafion®. However, it was obvious that a new sulfur-rich layer had been deposited, adding ohmic resistance to the MEA, which increased cell voltage and also pressed the MEA into anode flow passages, increasing pressure drop.

The existence of the sulfur layer was completely unexpected and suggested that, unless the cause for its formation could be understood and prevented, it had the potential to render PEM SDE technology infeasible.

3.2. Observations of colloidal sulfur and hydrogen sulfide formation

There were other observations that finally led to the solution of the problem. Sometimes the cell current was abruptly stopped after the cell had been operating. A couple of minutes later a cloud of colloidal sulfur appeared in the water/hydrogen separator. Then a couple of minutes after resuming the current, the contents of the separator began to clear.

Another observation was the odor of hydrogen sulfide, not SO_2, emitted by the water flowing out of the water/hydrogen separator. This was initially a surprise because some SO_2 was expected to cross the membrane from the anode to the cathode. Operating with the cathode pressure greater than the anode pressure decreased the appearance of colloidal sulfur in the separator and the odor of hydrogen sulfide in the effluent from the separator.

3.3. Observations on cell voltage

Figure 4 shows typical cell voltages as a function of current density for initial testing. The voltage at very low current density, not plotted here, is the reversible voltage for SDE, approximately 200 mV [19]. The kinetic over-potential term adds about 400 mV at 150 mA/cm^2 current density. At current densities greater than 150 mA/cm^2, there is a linear region resulting from ohmic-overpotential and above some higher current density, not shown in **Figure 4**, the

voltage increases sharply because of mass transfer over-potential. This last term is the result of mass transfer limitations; either the supply of reactants to the active catalyst sites is limiting, or diffusion of sulfuric acid product away from catalyst sites is limiting. In fact, for the present HyS electrolyzer, any mass transfer limitation was always the result of an inadequate supply of SO_2. The two lines in **Figure 4** show the linear regions for operation at ambient temperature and pressure and at 80°C and 4 atm for nominally identical MEAs. Note that increasing the temperature decreases both the slope and intercept of the line tracing the linear region. Typical intercepts for ambient operation and 80°C operation are 0.62 V and 0.58 V, respectively.

Cell voltages generally increased during early tests over the course of testing an MEA. **Figure 5** illustrates this trend for some ambient temperature and pressure operation. After placing a linear fit through data points with current densities greater than 150 mA/cm^2, it can be seen that all three data sets have the same intercept, 0.62 V. This behavior is consistent with an increasing internal electrical resistance of the MEA, which would be expected with an increasing layer of sulfur.

Inspection of cell polarization data like **Figure 4** and **Figure 5** showed an important simplification. For current densities greater than 150 mA/cm^2 and less than the current density for which mass transfer became important, which was not reached in these data sets, the plot could be approximated by an intercept and a slope. For most MEAs tested, the intercept was about 0.58 V for 80°C and 0.62 V for ambient temperature. The slope, which has units of ohm-cm^2, measured for initial testing of an MEA depended on membrane type and thickness and on catalyst loading. As testing progressed the slope increased because a sulfur layer of increasing thickness was adding electrical resistance to the cell, but the intercept, either 0.58 V or 0.62 V depending on temperature, usually remained the same.

3.4.Effect of SO_2 concentration in the anolyte

Figure 6 plots cell voltage for MEA 8 at four anolyte pressures; 1, 2, 3 and 4 bar. The corresponding SO_2 concentrations at 80°C and 30 wt% H_2SO_4 in the anolyte were estimated to be 0.14, 0.37, 0.61 and 0.85 molar, respectively, using the properties model described in [27]. The cell voltage for the highest concentration can be represented by a line with intercept 0.61 V and slope 0.49 Ω-cm^2, and no data points indicate mass transfer limitation. When the pressure was reduced to 3 bar, the line was unaffected except for current densities greater than 800 mA/cm^2, where there was mass transfer limitation. When the pressure was reduced to 2 bar, the line was unaffected except for current densities greater than 500 mA/cm^2, and when the pressure was reduced to 1 bar, the line was unaffected except for current densities above 250 mA/cm^2. This suggests that a certain concentration of SO_2 is necessary as a reactant for the anode reaction to proceed at a particular rate and the necessary concentration depends on current. Increasing the current increases the reaction rate and the necessary concentration of SO_2. If less than the necessary concentration is provided, the cell voltage increases because a reactant is limited and the anode overpotential term in Eqn. (4) becomes large. If a higher SO_2 concentration is provided, there is no effect on cell voltage at the current densities tested.

3.5.Hypothesis for formation of the sulfur layer

SO_2 dissolved in the anolyte crosses the membrane to the cathode under the action of two forces. First, a concentration gradient always drives SO_2 from the anode to the cathode. Second, SO_2 dissolved in water is transported by the flux of water through the membrane which can be in either direction. Water flux has three components. Electro-osmotic drag always drives water from the anode to cathode. The activity (concentration) gradient of water always drives water from the cathode to the anode because the anolyte is typically 30 wt% H_2SO_4 and 70 wt% water,

while pure water is supplied to the cathode. The pressure gradient across the membrane can drive water from higher to lower pressure, which can be chosen to be in either direction. The electrically driven anode reaction consumes SO_2 and therefore reduces the SO_2 concentration at the anode relative to the bulk stream concentration.

The first location where SO_2 can contact hydrogen gas in the presence of catalyst is at the interface between the membrane and the cathode. Two parasitic chemical reactions, shown below, are necessary to form elemental sulfur. The first reaction is energetically preferred because its standard Gibbs free energy change, $\Delta G°$ is more negative, and the reaction forms hydrogen sulfide. The second reaction, known as the Claus Reaction, is less energetically favorable and forms elemental sulfur.

$$SO_2(aq) + 3H_2(g) \rightarrow H_2S(aq) + 2H_2O(l), \quad \Delta G° = -201.4\ kJ/mol \tag{5}$$

$$SO_2(aq) + 2H_2S(aq) \rightarrow 3S(s) + 2H_2O(l), \quad \Delta G° = -117.9\ kJ/mol \tag{6}$$

This observation led to the hypothesis that limiting the concentration of SO_2 at the interface between the membrane and cathode would result in all SO_2 arriving at the interface being consumed in the first and less harmful reaction, leaving no SO_2 to participate in the second reaction. There are at least four ways to reduce the concentration of SO_2 at the interface.

1. Reduce the SO_2 concentration in the bulk anolyte.
2. Increase current density to consume more SO_2 at the anode. This decreases the concentration at the anode and membrane interface.
3. Increase the net water flux from cathode to the anode.
4. Decrease the permeability of the membrane to SO_2.

There are possible disadvantages to all four methods.

1. If SO_2 concentration is reduced enough cell voltage will increase, see **Figure 6**.

2. Increasing current density generates more hydrogen production from a given cell area but increases cell voltage.
3. A sufficiently high water flux from cathode to anode might interfere with hydrogen ion diffusion through the membrane and this would increase cell voltage.
4. A membrane that was less permeable to SO_2 might also be less permeable to hydronium ions.

3.6. Mapping cell operation to prevent sulfur formation

Inspection of **Figure 6** for MEA 8 suggests that higher concentrations of SO_2 in the anolyte allow higher current densities before cell operation becomes mass transfer limited. Therefore, the three current densities at the branch points in **Figure 6** were plotted against the corresponding SO_2 molarities in **Figure 7**. Also, five similar data points from testing MEA 29 were plotted. It should be noted that MEA 8 was tested with a previous design of the anolyte flowfield that was developed for higher anolyte flowrates. While there is significant scatter in the data, they suggest proportionality between SO_2 molarity and mass transfer limited current density. A line was plotted on the graph that passed through the origin and between the data points. The anode reaction was mass transfer limited for points below the line. The further below the line, the higher the cell voltage, but the less likely formation of sulfur is. For points above the line the anode reaction is not mass transfer limited. Moving further above the line does not change the cell voltage but it was hypothesized that sulfur formation is more likely and occurs faster. **Figure 8** plots where the other MEAs were operated on the operating map. Note that the weekend period during the first longevity test, when MEA 12 was stored in SO_2-saturated anolyte, was the MEA 12 data point furthest from the dividing line on **Figure 8** and

also the period when the fastest increase in cell voltage occurred. Note also that the data discussed in the preceding paragraph pertain to the particular catalysts, flowfields, flowrates and membranes that were studied. However, the method could be applied to any SDE cell.

The data for the points labeled "Button Cell" were generated in a different, very small (i.e., button cell) electrolyzer used to test candidate membranes and various catalyst compositions. It only operated at atmospheric pressure and 60°C and therefore the anolyte could not have high SO_2 molarity. Significantly, the button cell electrolyzer never developed a sulfur layer at the cathode.

3.7.New operating procedure to prevent sulfur formation

A new operating envelope or procedure was proposed and tested, which was to limit operation at all times just below the dividing line on **Figure 7** and **Figure 8** so that cell voltage is, at most, slightly increased and sulfur formation is greatly reduced or eliminated. It is important to stay below the line not only during steady state operation but also during startup and shutdown.

At startup, this was accomplished by loading fresh anolyte with no SO_2. The power supply was used to impress 0.9 V across the cell. Anolyte and cell were heated to the desired temperature. The 0.9-V potential is insufficient to accomplish conventional water electrolysis which would generate oxygen, but enough to consume SO_2 once it is added or any traces of SO_2 left from previous operation. SO_2 was slowly added while verifying that the transition conditions remained below the dividing line in **Figure 7** and **Figure 8**. This increased anolyte pressure, concentration of SO_2 and current density. Results from [27] were used to calculate SO_2 concentration from anolyte temperature and pressure. When the target current was reached, power supply operation was changed to current control. If an increase in SO_2 concentration did

not decrease cell voltage, then the SO_2 concentration was decreased until the first indication of SO_2 limited operation was reached.

Shutdown of the facility was accomplished with the following steps. While current and operating temperatures were maintained, the feed of SO_2 was stopped which slowly decreased anolyte pressure as the SO_2 was consumed. Venting SO_2 vapor to accelerate the pressure decrease was not normally done because it caused gas bubble formation in the anolyte pump. Pressure reduction decreased the concentration of SO_2 in the anolyte and caused cell voltage to increase. When the cell voltage increased to 0.9 V, the power supply automatically switched to voltage control at which time cell current decreased as SO_2 was consumed. Once anolyte pressure decreased to atmospheric, the power supply and the anolyte pump were simultaneously de-energized while allowing the cathode water flush to continue. Then the valve at the outlet of the anolyte tank was closed and the anode of the cell was flushed with deionized water. Both sides of the cell were stored in water.

3.8.Normalization of cell voltage

To allow better comparison of data collected over a wide range of conditions, a method was developed to normalize cell voltage with respect to current density and temperature. Normalization of cell voltage was accomplished by dividing the slope of the linear part of the voltage response by the slope of a standard MEA. Based on an earlier report [14] the standard response for ambient conditions was defined to be the following, where *E* and *i* are cell voltage and current density (A/cm^2), respectively.

$$E = 0.62\,V + \left(0.67\ ohm - cm^2\right) i \tag{7}$$

The standard response for 80°C was defined to be the following.

$$E = 0.58\,V + \left(0.42\ ohm - cm^2\right) i \tag{8}$$

Note that both the intercept and slope decrease when the temperature increases from ambient to 80°C. Implementation of normalization for ambient and 80°C used the following two equations,

$$E_{norm} = \left(E_{meas} - 0.62\,V\right)/\left(0.67i\right) \text{ for ambient operation} \quad (9)$$

$$E_{norm} = \left(E_{meas} - 0.58\,V\right)/\left(0.42i\right) \text{ for 80°C operation} \quad (10)$$

where E_{norm} is the normalized cell voltage, while E_{meas} if the experimentally measured cell voltage.

The normalization process compensates for temperature and current density, and can be thought of as comparing the ohmic loss of an MEA to the baseline ohmic loss. When the normalized voltage is 1.2, the ohmic loss is 20% higher than baseline.

Another method for comparing cell voltages is to use Area Specific Resistance (ASR), which was used by Idaho National Laboratory (INL) in their high temperature steam electrolysis (HTE) work [28]. INL defines ASR as follows.

$$ASR = \left(E_{op} - E_{Nernst}\right)/i \quad (11)$$

The terms E_{op} and E_{Nernst} are the operating voltage and the Nernst potential, respectively. ASR has units of ohm-cm^2. An altered form of eqn 11 was sometimes used for HyS results.

$$ASR_{HyS} = \left(E_{meas} - E_0\right)/i \quad (12)$$

The term E_0 is the intercept for eqns. (7) and (8), interpolated for temperature.

Equations (9) and (10) were used to normalize cell voltage from the MEA 12 longevity run and eqn. (12) was used to calculate the ASR, as shown in **Figure 9**. Operating conditions were 80°C and 4 atm. Normalized cell voltage was initially about 1.0, implying good performance. After the weekend, it increased to 1.4, so that ohmic resistance had increased by 40%. At the end of the run ohmic resistance was 90% higher than originally. ASR is a function

of temperature, generally decreasing with increasing temperature. For comparison, INL reported ASR ranging from 0.7 to 1.3 ohm-cm^2 for operation of their HTE at 800°C.

3.9. Results of applying the sulfur elimination method

The method for eliminating sulfur was most successfully applied during the testing of MEAs 36 and 37, the final MEAs tested in the experiment series. While there were equipment issues during the testing of MEA 36, subsequent analyses of both MEAs indicated no sulfur formation. Test results for MEA 37 follow.

MEA 37 was tested continuously over a ten-day period. Previous software and hardware improvements were successful in fine tuning the facility for mostly unattended operation. Other than minor pressure variations, testing was uneventful and cell voltage was steady, as shown in **Figure 10**. SO_2 molarity in the figure was computed based on pressure, temperature, and acid concentration [27]. There was a slight downward trend in hydrogen sulfide concentration, which may actually have been an artifact of column aging in the gas chromatograph. At the end of testing, MEA 37 appeared to be in pristine condition. An SEM analysis, **Figure 11**, as well as energy dispersive x-ray spectra, not shown, showed no sulfur layer.

Measured hydrogen flowrate was steady at 0.50±0.02 mol/hr, which is 98%±4% of theoretical for the cell current. Measured pressure in the anolyte tank was 0.76 barg (11 psig), pressure drop for anolyte flow through the cell was 0.14 bar (2 psid) and cathode pressure was 1.86 barg (27 psig). Cathode pressure was maintained higher to increase water flux from the cathode to the anode and to limit diffusion of SO_2 from anode to cathode. The hydrogen product contained 0.06 mol % hydrogen sulfide. Because three moles of hydrogen are required to form one mole of hydrogen sulfide, 0.18% of the hydrogen product was consumed by the parasitic

reaction. In a future commercial plant, the hydrogen sulfide would be separated from the product hydrogen and oxidized to SO_2 for reuse in the process.

The earlier discovery of the sulfur rich layer in MEA 12 following its longevity test was considered such a potentially devastating problem, that proof of the validity of the new operating envelope with the MEA 36 and MEA 37 tests was a significant achievement. Based on this work, a patent was applied for and granted, prescribing operating conditions under which formation of the sulfur layer in the MEA could be prevented [17].

3.10. Trends for cell voltage

Figure 12 shows that cell voltage increases with increasing sulfuric acid concentration. There are two major reasons for this: (1) the Nafion® membrane begins to dehydrate, reducing its ability to transfer hydronium ions; and (2) the solution becomes more viscous, which reduces mobility of reactants and products. Because of reduced mobility, the local concentrations of reactants are decreased and the local concentration of product is increased. This increases the Nernst potential. This effect may be less important with a non-Nafion® membrane. **Figure 13** shows that decreasing partial pressure of SO_2 in the anolyte increases cell voltage, when SO_2 is the limiting reactant. As was discussed before, increases in SO_2 concentration beyond a certain point do not decrease voltage, but generate elemental sulfur and increased quantities of parasitic reaction product hydrogen sulfide. **Figure 14** shows that increasing cell temperature decreases cell voltage, because reaction rate increases and viscosity decreases. Reactants and products can move to and from catalyst active sites more easily. **Figure 15** shows that increasing anolyte flow decreases cell voltage, up to a point, because it improves mass transfer. However, increasing flowrate decreases per-pass conversion.

Most of the 37 MEAs tested had anodes and cathodes containing platinized carbon with platinum loadings ranging from 0.8 to 1.8 mg/cm^2. For ambient temperature operation, higher platinum loading decreased initial cell voltage. However for operation at 80°C, platinum loading made little difference in initial cell voltage. Cell voltage was lowest for a few hours after startup, and then increased to a value that was steady or slowly increasing depending on whether a sulfur layer was being formed.

4. Conclusions

SDE has promise as a source of bulk hydrogen that does not contribute to climate change and that can be operated sustainably when coupled with high temperature decomposition of sulfuric acid in a HyS cycle driven by a renewable heat source. It can also be used in an open circuit process for co-production of sulfuric acid from an SO_2 source like a power plant flue gas or ore smelter off-gas. There are three primary technical obstacles to commercialization of SDE: 1) capital cost of the electrolyzers; 2) frequency of MEA replacement; and 3) power cost compared to the value of the products. The work reported here contributes to the resolution of all three issues. The most important result was the resolution of the sulfur formation problem. In the first series of tests reported here, sulfur was observed to accumulate inside the MEA. This increased cell voltage, which increases power cost, but, more importantly, destroyed the MEA in only hundreds of hours of operation. That would necessitate replacement of the MEA in commercial applications at a frequency that would prevent SDE from becoming economically viable. A commercial application would require MEAs to last tens of thousands of hours. This research developed and verified an operating procedure to prevent sulfur formation in the MEA that led to the award of a patent. The issue of capital cost was addressed by developing a thin

cell that borrows from conventional PEM fuel cell designs and components, that can be stacked, and which has good per-pass conversion of SO_2. This means future improvements in PEM fuel cell technology, for which the development effort is much greater than for SDE, could be leveraged to lower capital cost even further. The cell also allows operation at practical current densities, which results in reasonable values of the MEA total area required for a given application. This work demonstrated that the electron efficiency for hydrogen generation is close to 100%, and the cell voltage is much lower than for conventional electrolysis. Data were collected which would allow process optimization, at least for the base case of platinized carbon catalyst on Nafion® membrane. For example, it is commercially desirable to produce high concentration sulfuric acid but that requires more electrical power per mole of acid generated. Data presented here could be used for optimization.

Because of funding constraints, the tests reported here were conducted almost exclusively with Nafion® membranes. However, as was mentioned in Section 1.2, the use of PBI membranes has the potential to decrease cell voltage and increase product acid concentration. Current work at SRNL on SDE includes experiments with acid-doped PBI membranes.

Acknowledgements

The authors gratefully acknowledge funding from the US Department of Energy's Office of Nuclear Energy under the Nuclear Hydrogen Initiative, for which Mr. Carl Sink was the program manager, and thank Dr. William A. Summers, who led SRNL's HyS development effort for his guidance and support. SRNL is operated for the DOE's Office of Environmental

578 Management (DOE-EM) by Savannah River Nuclear Solutions, LLC under contract number DE-
579 A C09-08SR22470.

580

References

[1] Funk JE, Reinstrom RM. Energy requirements in the production of hydrogen from water. *l&EC Process Design and Development.* July 1966 1966;5(3):336-342.

[2] Brecher LE, Spewock S, Warde CJ. The Westinghouse Sulfur Cycle for the thermochemical decomposition of water. *International Journal of Hydrogen Energy.* 1977;2(1):7-15.

[3] Brecher LE, Wu CK; Westinghouse Electric Corp., assignee. Electrolytic decomposition of water. US patent 3888750. June 10, 1975.

[4] Farbman GH. *Conceptual design of an integrated nuclear hydrogen production plant using the sulfur cycle water decomposition system.* Westinghouse Electric Corp., Astronuclear Lab.; NASA Contractor Report, NASA-CR-134976. April 1, 1976.

[5] Lu WTP, Ammon RL, Parker GH. *A Study on the Electrolysis of Sulfur Dioxide and Water for the Sulfur Cycle Hydrogen Production Process; final report prepared for The Jet Propulsion Laboratory, Contract No. 955380.* Westinghouse Electric Corp., Advanced Energy Systems Division; AESD-TME-3043. July 1980.

[6] Lu PWT, Ammon RL. An Investigation of Electrode Materials for the Anodic Oxidation of Sulfur Dioxide in Concentrated Sulfuric Acid. *Journal of The Electrochemical Society.* December 1, 1980 1980;127(12):2610-2616.

[7] Lu PWT, Garcia ER, Ammon RL. Recent developments in the technology of sulfur dioxide depolarized electrolysis. *J. Appl. Electrochem.* 1981;11(3):347-355.

[8] Lu PWT, Ammon RL. Sulfur dioxide depolarized electrolysis for hydrogen production: development status. *International Journal of Hydrogen Energy.* 1982;7(7):563-575.

[9] Parker GH. *Solar Thermal Hydrogen Production Process: Final Report, January 1978-December 1982.* Westinghouse Electric Corp., Advanced Energy Systems Division; DOE/ET/20608-1. January 21, 1983.

[10] Lu PWT. Technological aspects of sulfur dioxide depolarized electrolysis for hydrogen production. *International Journal of Hydrogen Energy.* 1983;8(10):773-781.

[11] Cólon-Mercado HR, Hobbs DT. Catalyst evaluation for a sulfur dioxide-depolarized electrolyzer. *Electrochem. Commun.* 2007;9(11):2649-2653.

[12] Elvington MC, Colón-Mercado H, McCatty S, Stone SG, Hobbs DT. Evaluation of proton-conducting membranes for use in a sulfur dioxide depolarized electrolyzer. *Journal of Power Sources.* 2010;195(9):2823-2829.

[13] Cólon-Mercado HR, Elvington MC, Steimke JL, Steeper TJ, Herman DT, Gorensek MB, et al. Recent Advances in the Development of the Hybrid Sulfur Process for Hydrogen Production. *Nuclear Energy and the Environment.*ACS Symposium Series Vol 1046: American Chemical Society; 2010:141-154.

[14] Steimke J, Steeper T. *Phase I Single Cell Electrolyzer Test Results.* Savannah River National Laboratory; WSRC-STI-2008-00231. August 5, 2008.

[15] Steimke JL, Steeper TJ, Herman DT, Cólon-Mercado HR, Elvington MC. *Method to prevent sulfur accumulation inside Membrane Electrode Assembly.* Savannah River National Laboratory; SRNL-STI-2009-00134. June 22, 2009.

[16] Steimke JL, Steeper TJ, Herman DT, Cólon-Mercado HR. *Closeout Report for Hybrid Sulfur Single Cell Test Facility.* Savannah River National Laboratory. 2010.

[17] Steimke JL, Steeper TJ, Herman DT; Savannah River Nuclear Solutions, LLC, assignee. Method to prevent sulfur accumulation in membrane electrode assembly. US patent 8,709,229 B2. April 29, 2014.

[18] Staser JA, Weidner JW. Effect of Water Transport on the Production of Hydrogen and Sulfuric Acid in a PEM Electrolyzer. *J. Electrochem. Soc.* 2009;156(1):B16-B21.

[19] Staser JA, Gorensek MB, Weidner JW. Quantifying Individual Potential Contributions of the Hybrid Sulfur Electrolyzer. *Journal of The Electrochemical Society.* 2010;157(6):B952-B958.

[20] Stone S, McPheeters C, Staser J, Jayakumar JV, Weidner JW. Gas-Phase Hybrid Sulfur Electrolyzer Stack. *ECS Transactions.* 2011;35(37):23-33.

[21] Jayakumar JV, Gulledge A, Staser JA, Kim C-H, Benicewicz BC, Weidner JW. Polybenzimidazole Membranes for Hydrogen and Sulfuric Acid Production in the Hybrid Sulfur Electrolyzer. *ECS Electrochemistry Letters.* January 1, 2012 2012;1(6):F44-F48.

[22] Kriek RJ, Van Ravenswaay JP, Potgieter M, Calitz A, Lates V, Björketun M, et al. SO2 - An indirect source of energy. *The Journal of The Southern African Institute of Mining and Metallurgy.* 2013;113(8):593-604.

[23] Xue L, Zhang P, Chen S, Wang L, Wang J. Sensitivity study of process parameters in membrane electrode assembly preparation and SO_2 depolarized electrolysis. *International Journal of Hydrogen Energy.* 2013;38(25):11017-11022.

[24] Peach R, Krieg HM, Krüger AJ, van der Westhuizen D, Bessarabov D, Kerres J. Comparison of ionically and ionical-covalently cross-linked polyaromatic membranes for SO_2 electrolysis. *International Journal of Hydrogen Energy.* 2014;39(1):28-40.

[25] Allen JA, Rowe G, Hinkley JT, Donne SW. Electrochemical aspects of the Hybrid Sulfur Cycle for large scale hydrogen production. *International Journal of Hydrogen Energy.* 2014;39(22):11376-11389.

[26] Xue L, Zhang P, Chen S, Wang L. Pt-based bimetallic catalysts for SO_2-depolarized electrolysis reaction in the hybrid sulfur process. *International Journal of Hydrogen Energy.* 2014;39(26):14196-14203.

[27] Gorensek MB, Staser JA, Stanford TG, Weidner JW. A thermodynamic analysis of the SO_2/H_2SO_4 system in SO_2-depolarized electrolysis. *International Journal of Hydrogen Energy.* 2009;34(15):6089-6095.

[28] O'Brien JE, Stoots CM, Herring JS, Condie KG, Housley GK. *The high-temperature electrolysis program at the Idaho National Laboratory: observations on performance degradation.* Idaho National Laboratory; INL/CON-09-15564. June 2009.

List of Figure Captions

697 Figure 12 Effect of acid concentration on voltage.

698
699

700 Figure 13 Effect of partial pressure of SO_2 on MEA 31.

701
702

703 Figure 14 Effect of temperature on voltage, MEA 28.

704
705

706 Figure 15 Effect of flowrate on voltage.

707

List of Table Captions

Table 1 Characteristics of the MEAs tested in the SRNL SDE cell.

Figure 1

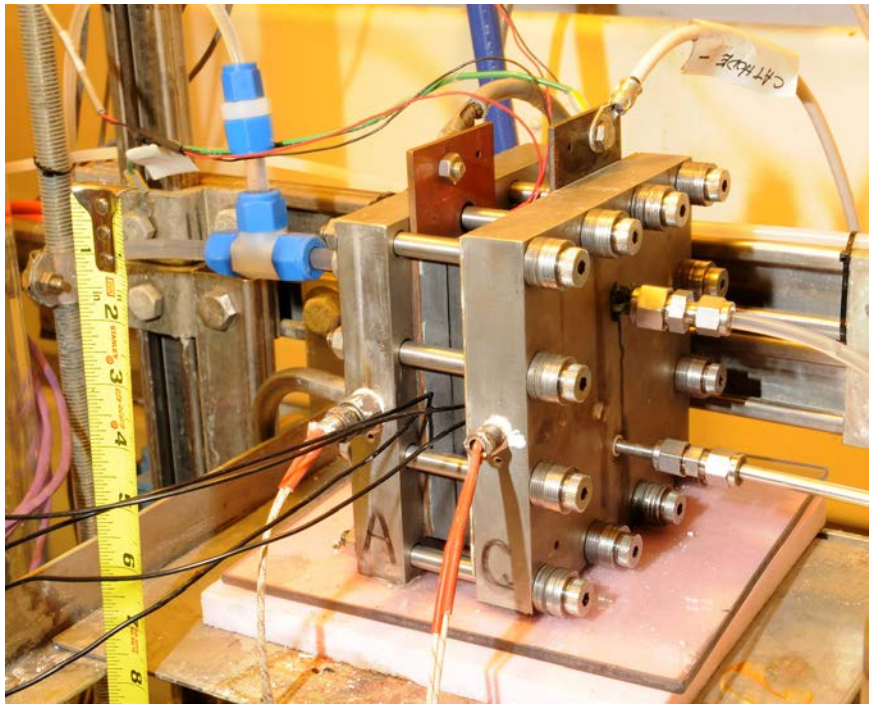

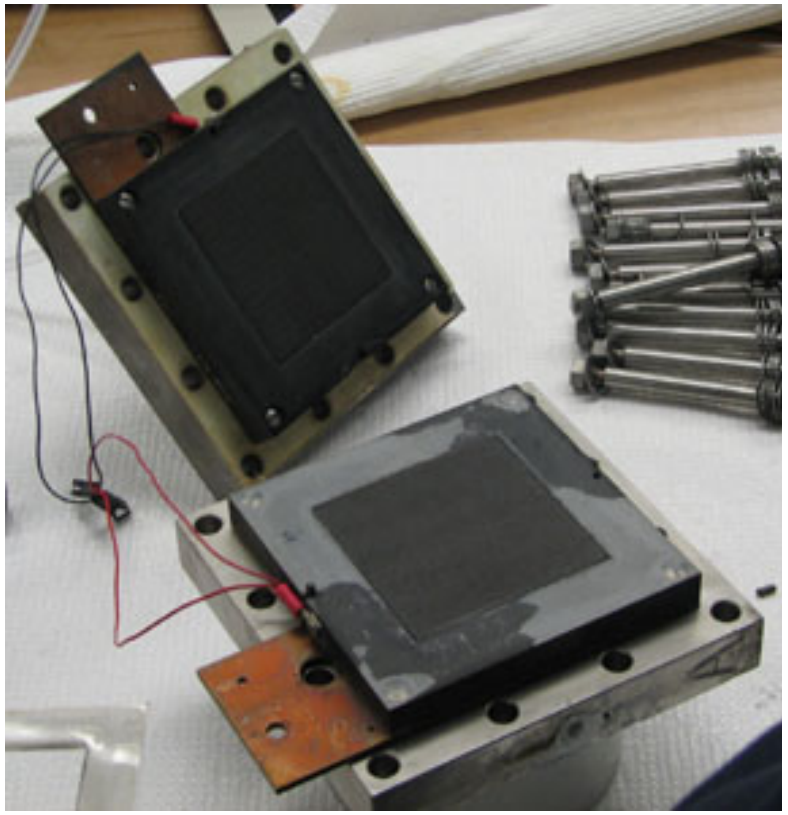

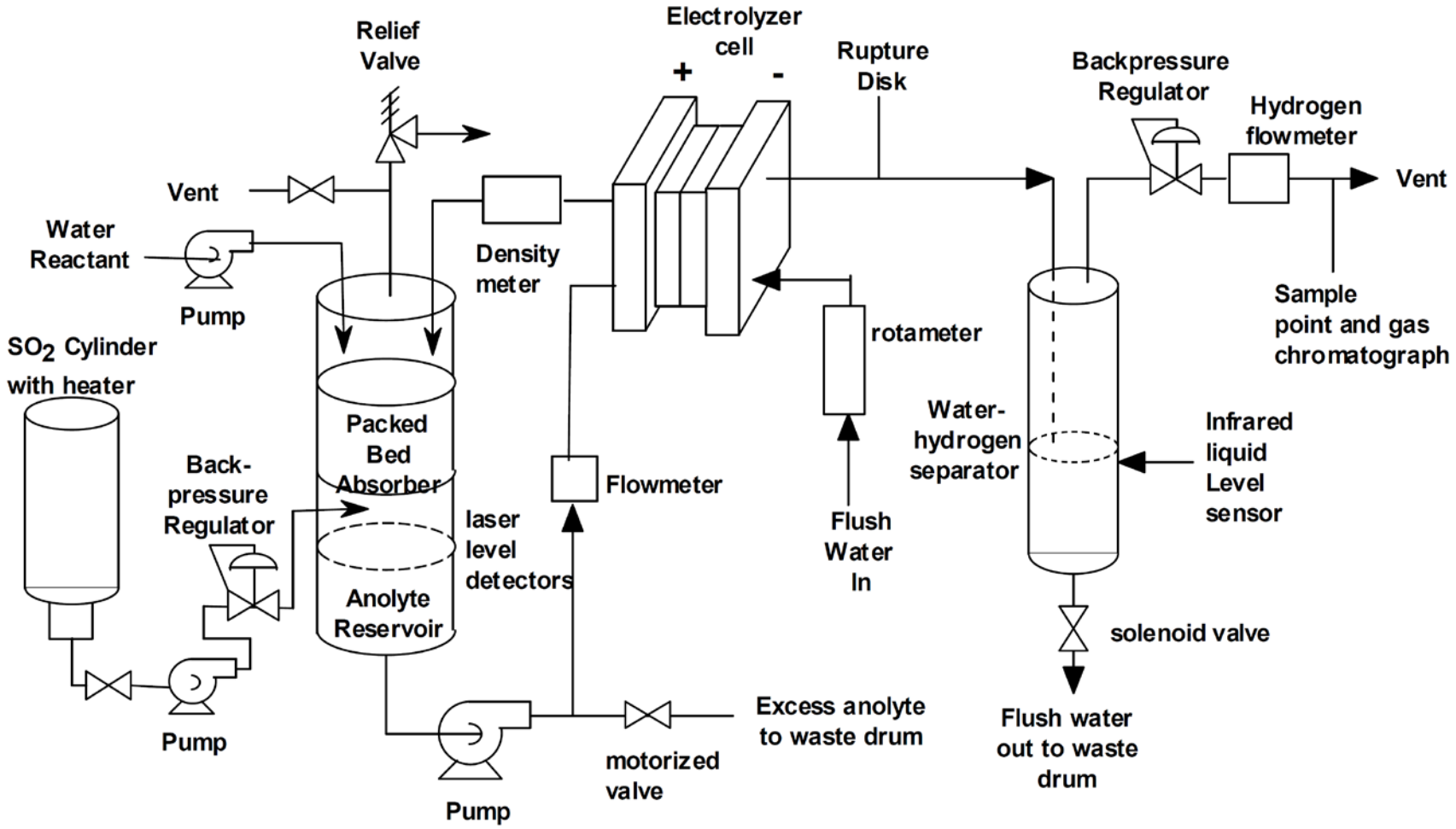
Relief
Valve
Electrolyzer
cell
+
-
Rupture
Disk
Backpressure
Regulator
Hydrogen
flowmeter
Vent
Vent
Water
Reactant
Pump
Density
meter
rotameter
Sample
point and gas
chromatograph
SO_2 Cylinder
with heater
Packed
Bed
Absorber
Water-
hydrogen
separator
Infrared
liquid
Level
sensor
Back-
pressure
Regulator
Flowmeter
laser
level
detectors
Flush
Water
In
Anolyte
Reservoir
solenoid valve
Pump
Excess anolyte
to waste drum
Flush water
out to waste
drum
motorized
valve
Pump

Figure 2

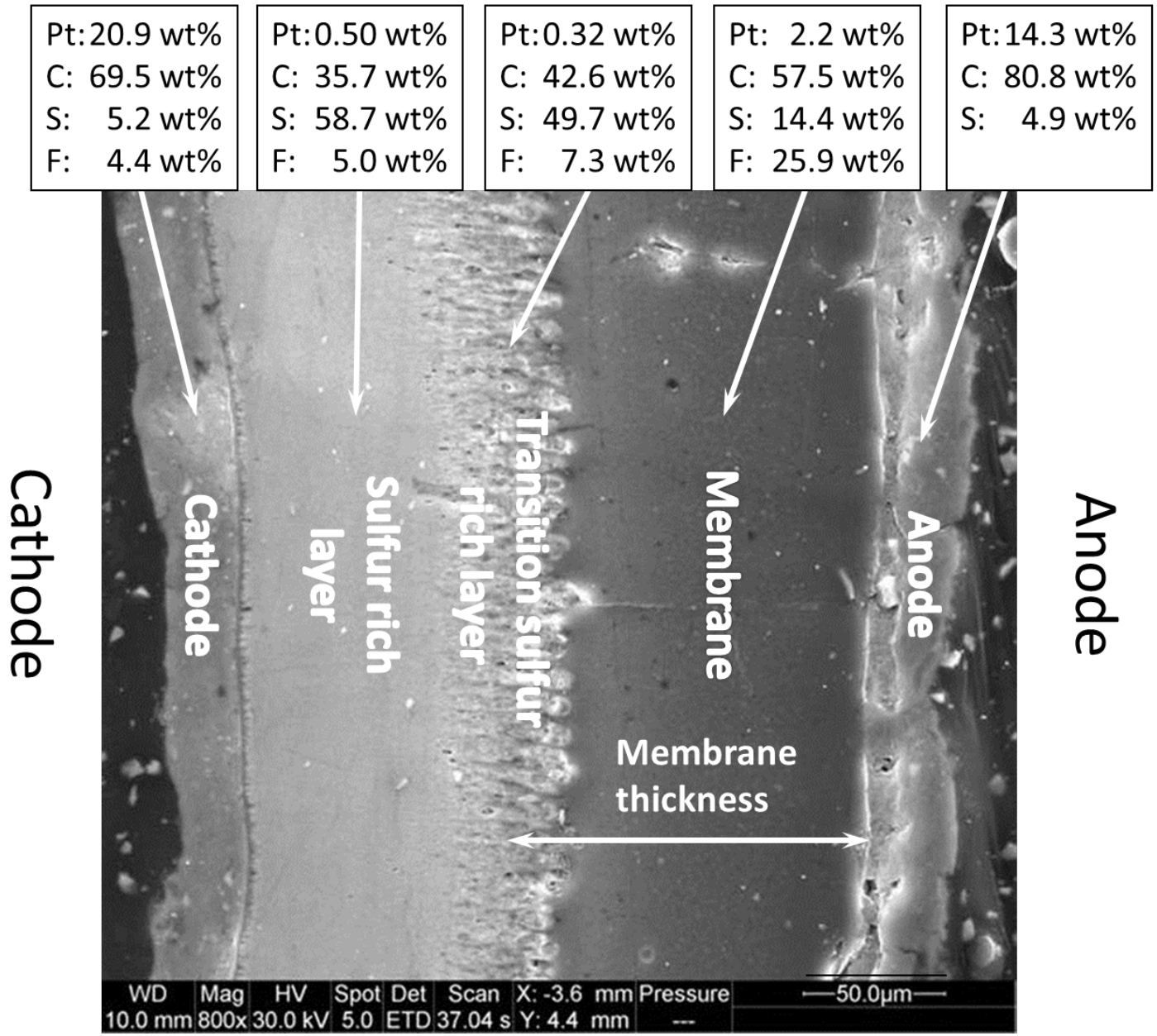
Pt: 20.9 wt%
C: 69.5 wt%
S: 5.2 wt%
F: 4.4 wt%
Pt: 0.50 wt%
C: 35.7 wt%
S: 58.7 wt%
F: 5.0 wt%
Pt: 0.32 wt%
C: 42.6 wt%
S: 49.7 wt%
F: 7.3 wt%
Pt: 2.2 wt%
C: 57.5 wt%
S: 14.4 wt%
F: 25.9 wt%
Pt: 14.3 wt%
C: 80.8 wt%
S: 4.9 wt%
Cathode
Cathode
Sulfur rich layer
Transition sulfur rich layer
Membrane
Anode
Anode
Membrane thickness
WD 10.0 mm
Mag 800x
HV 30.0 kV
Spot 5.0
Det ETD
Scan 37.04 s
X: -3.6 mm
Y: 4.4 mm
Pressure ---
50.0µm

Figure 3

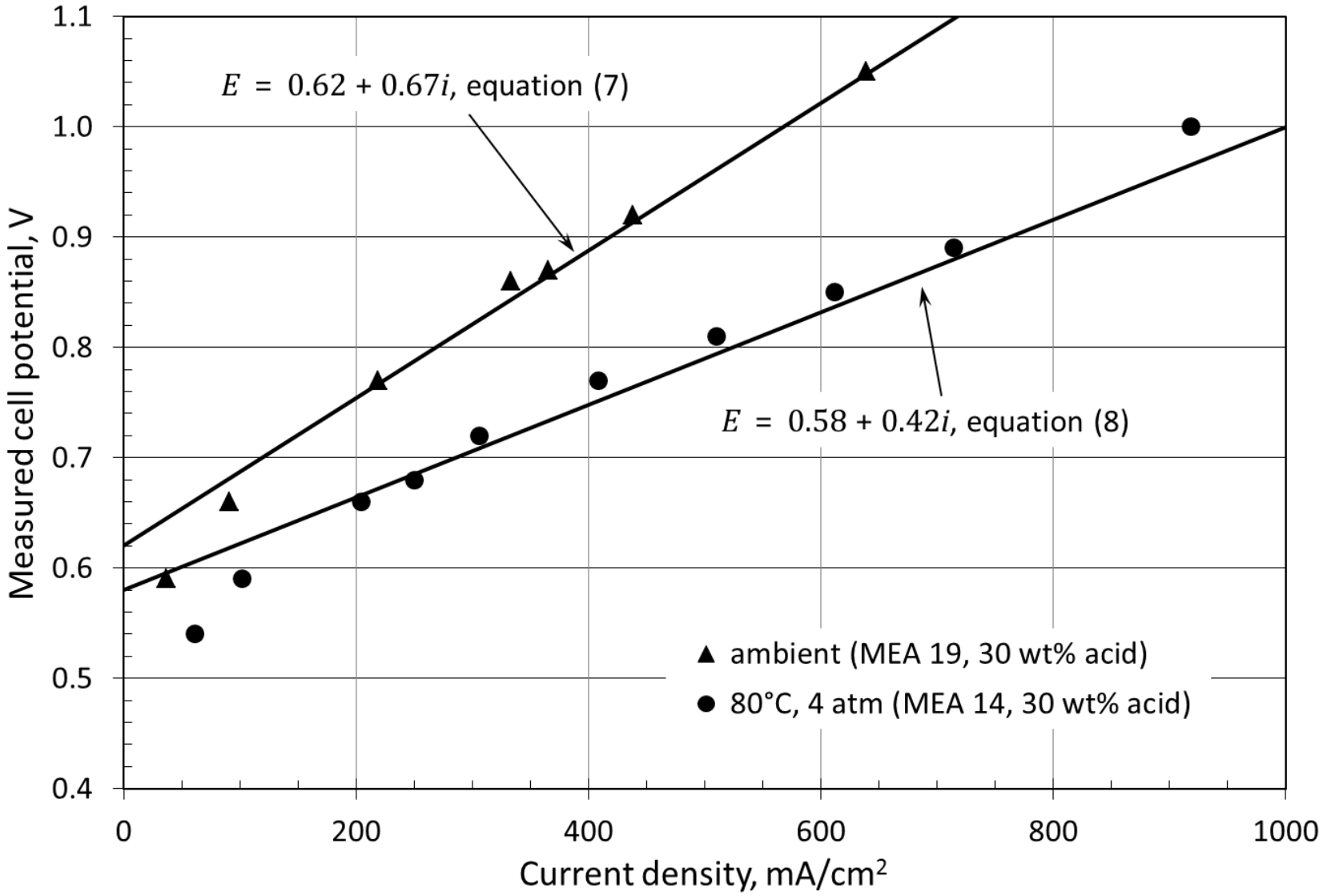
1.1
1.0
0.9
0.8
0.7
0.6
0.5
0.4
Measured cell potential, V
0
200
400
600
800
1000
Current density, mA/cm²
E = 0.62 + 0.67i, equation (7)
E = 0.58 + 0.42i, equation (8)
ambient (MEA 19, 30 wt% acid)
80°C, 4 atm (MEA 14, 30 wt% acid)

Figure 4

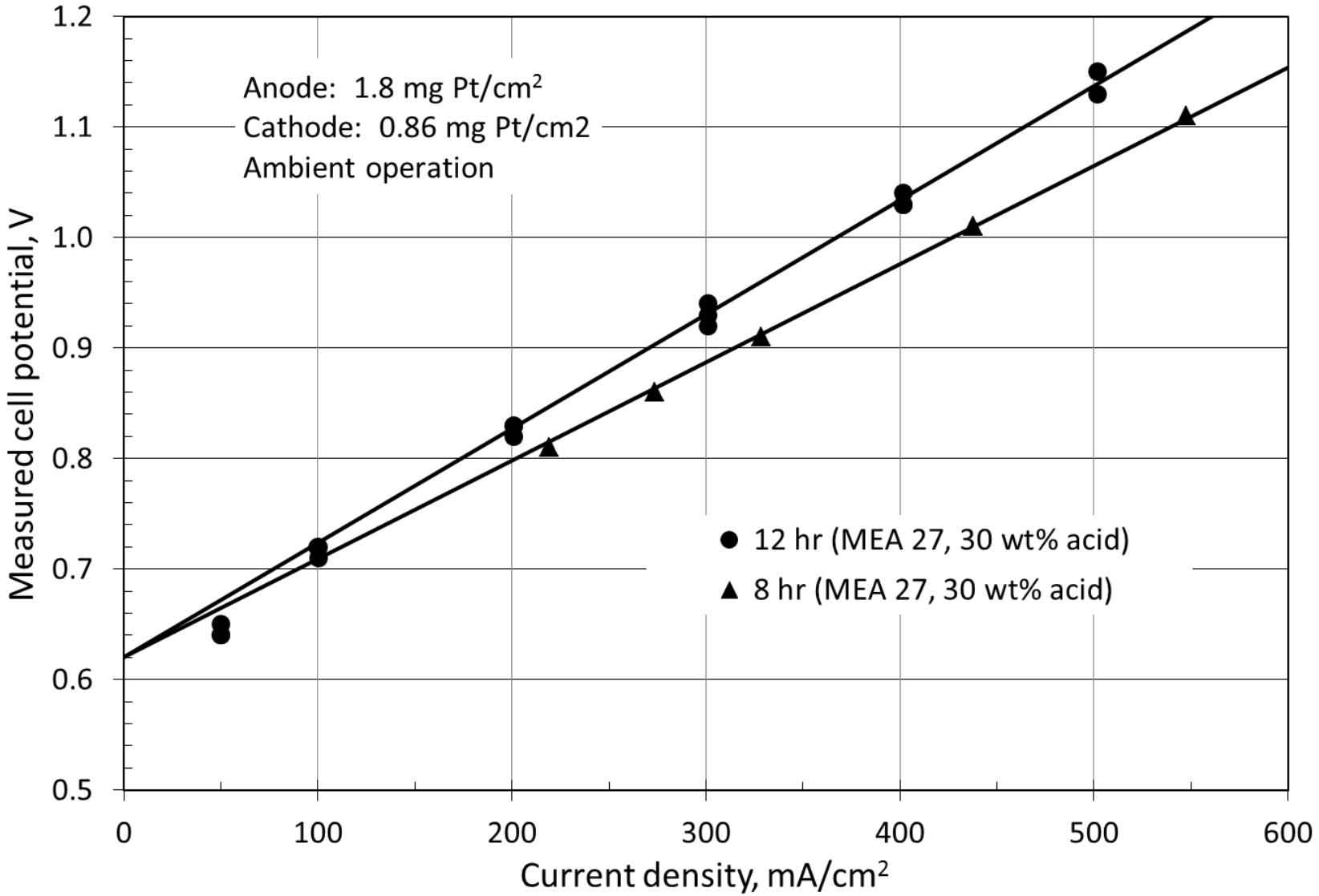
Anode: 1.8 mg Pt/cm²
Cathode: 0.86 mg Pt/cm2
Ambient operation
12 hr (MEA 27, 30 wt% acid)
8 hr (MEA 27, 30 wt% acid)
Measured cell potential, V
Current density, mA/cm²
1.2
1.1
1.0
0.9
0.8
0.7
0.6
0.5
0
100
200
300
400
500
600

Figure 5

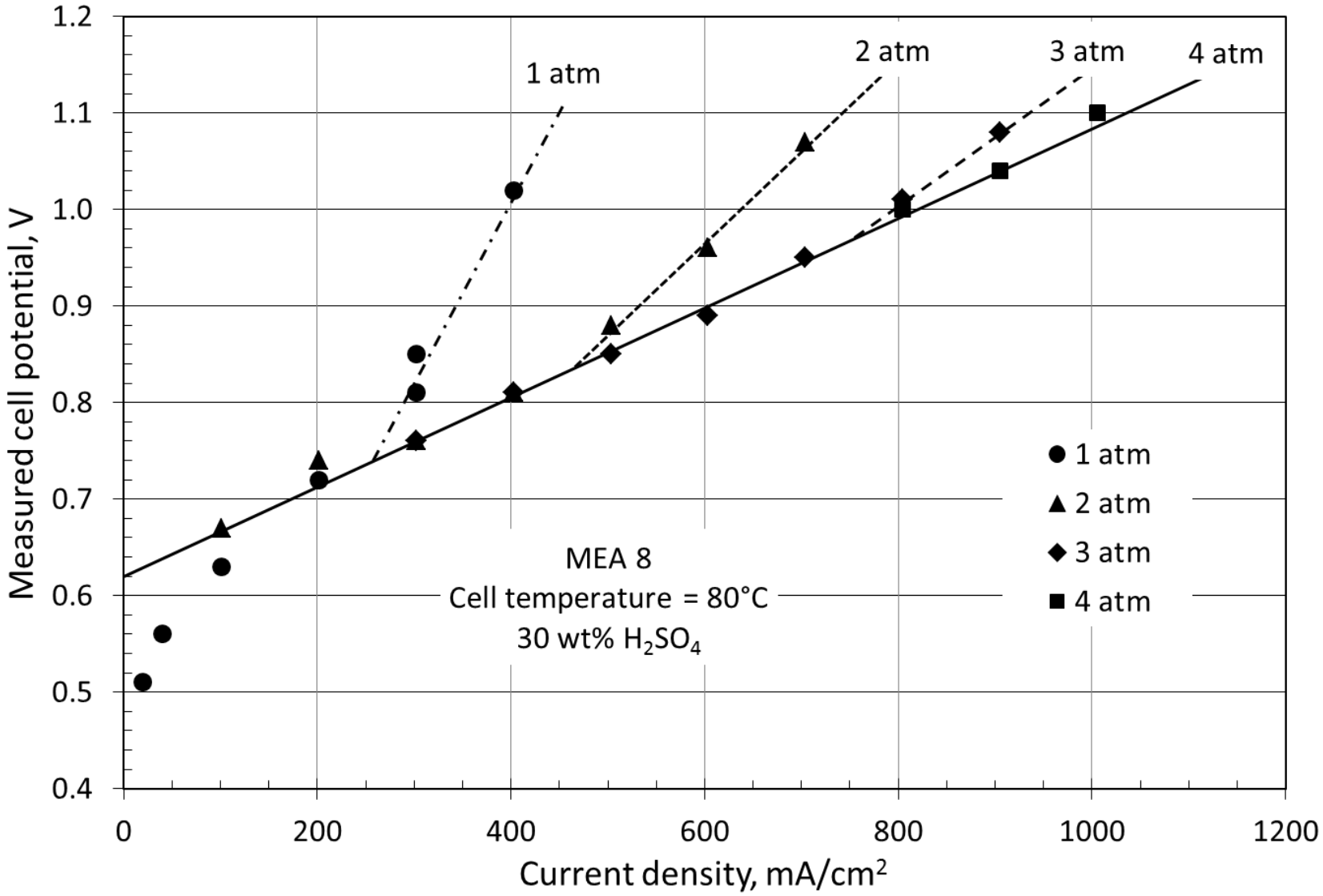
1.2
1.1
1.0
0.9
0.8
0.7
0.6
0.5
0.4
Measured cell potential, V
0
200
400
600
800
1000
1200
Current density, mA/cm2
1 atm
2 atm
3 atm
4 atm
MEA 8
Cell temperature = 80°C
30 wt% H2SO4
1 atm
2 atm
3 atm
4 atm

Figure 6

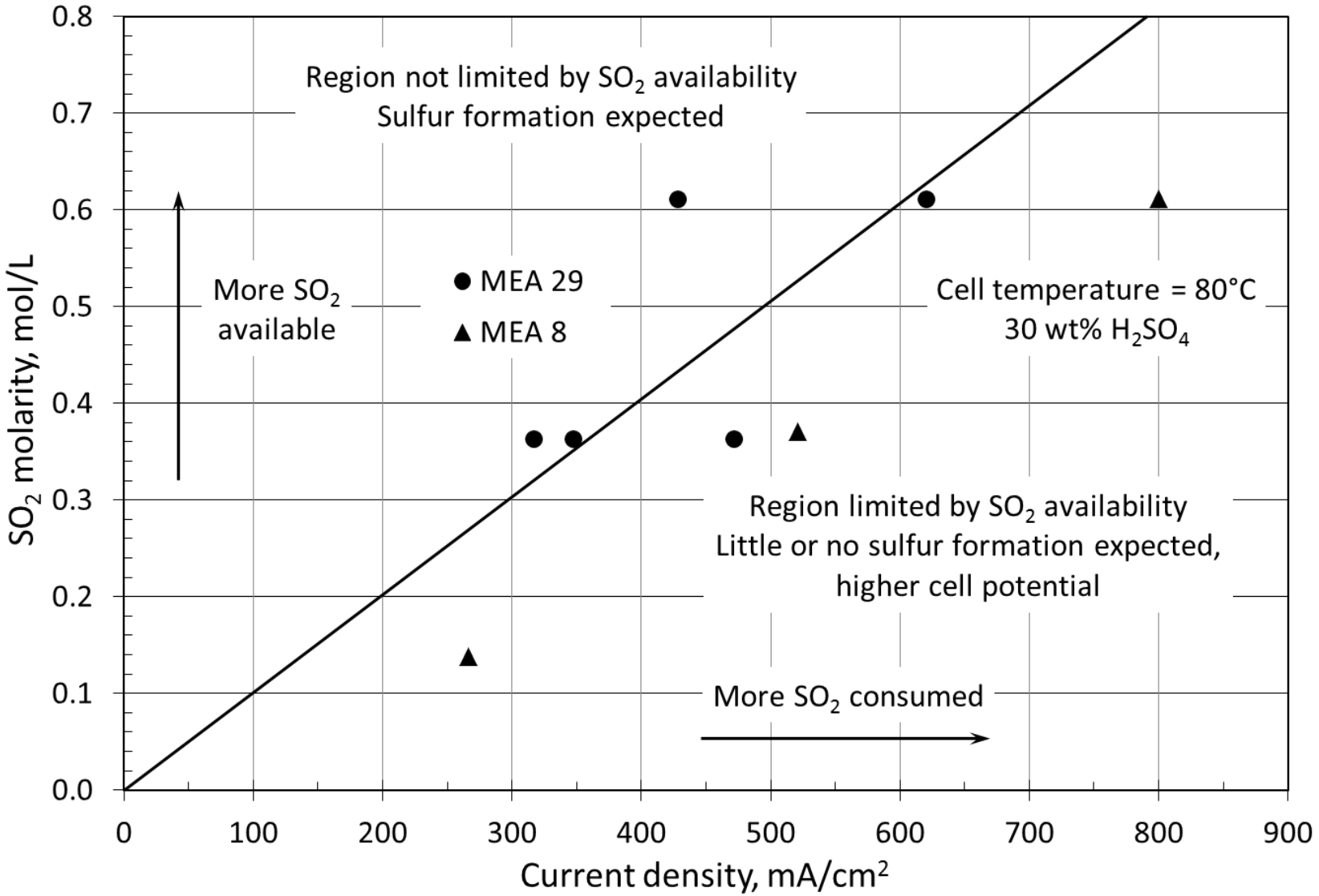
Region not limited by SO_2 availability
Sulfur formation expected
More SO_2 available
MEA 29
MEA 8
Cell temperature = 80°C
30 wt% H_2SO_4
Region limited by SO_2 availability
Little or no sulfur formation expected,
higher cell potential
More SO_2 consumed
SO_2 molarity, mol/L
Current density, mA/cm^2
0.0
0.1
0.2
0.3
0.4
0.5
0.6
0.7
0.8
0
100
200
300
400
500
600
700
800
900

Figure 7

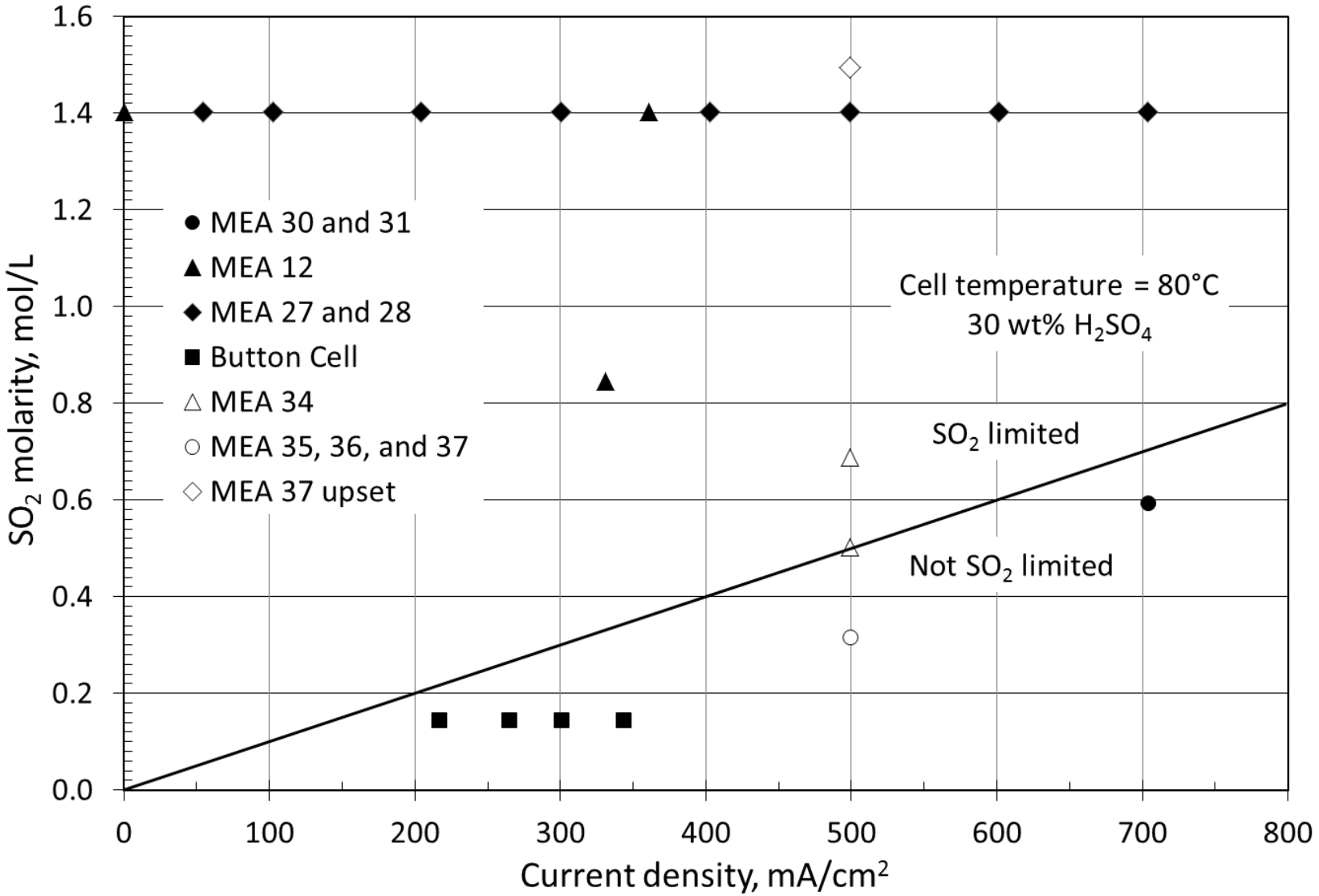
1.6
1.4
1.2
1.0
0.8
0.6
0.4
0.2
0.0
SO2 molarity, mol/L
0
100
200
300
400
500
600
700
800
Current density, mA/cm2
MEA 30 and 31
MEA 12
MEA 27 and 28
Button Cell
MEA 34
MEA 35, 36, and 37
MEA 37 upset
Cell temperature = 80°C
30 wt% H2SO4
SO2 limited
Not SO2 limited

Figure 8

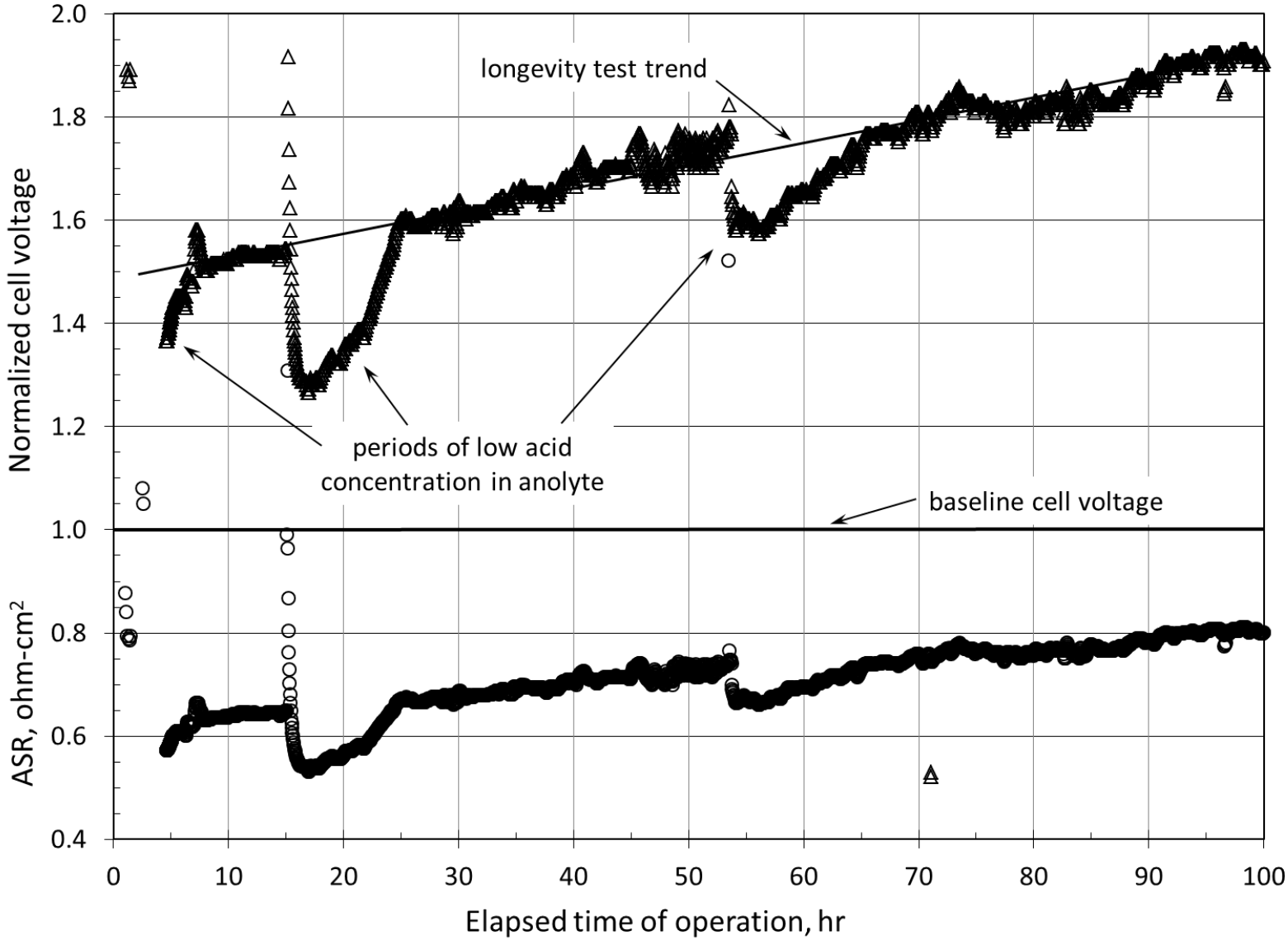
longevity test trend
periods of low acid concentration in anolyte
baseline cell voltage
Normalized cell voltage
ASR, ohm-cm²
Elapsed time of operation, hr
2.0
1.8
1.6
1.4
1.2
1.0
0.8
0.6
0.4
0
10
20
30
40
50
60
70
80
90
100

Figure 9

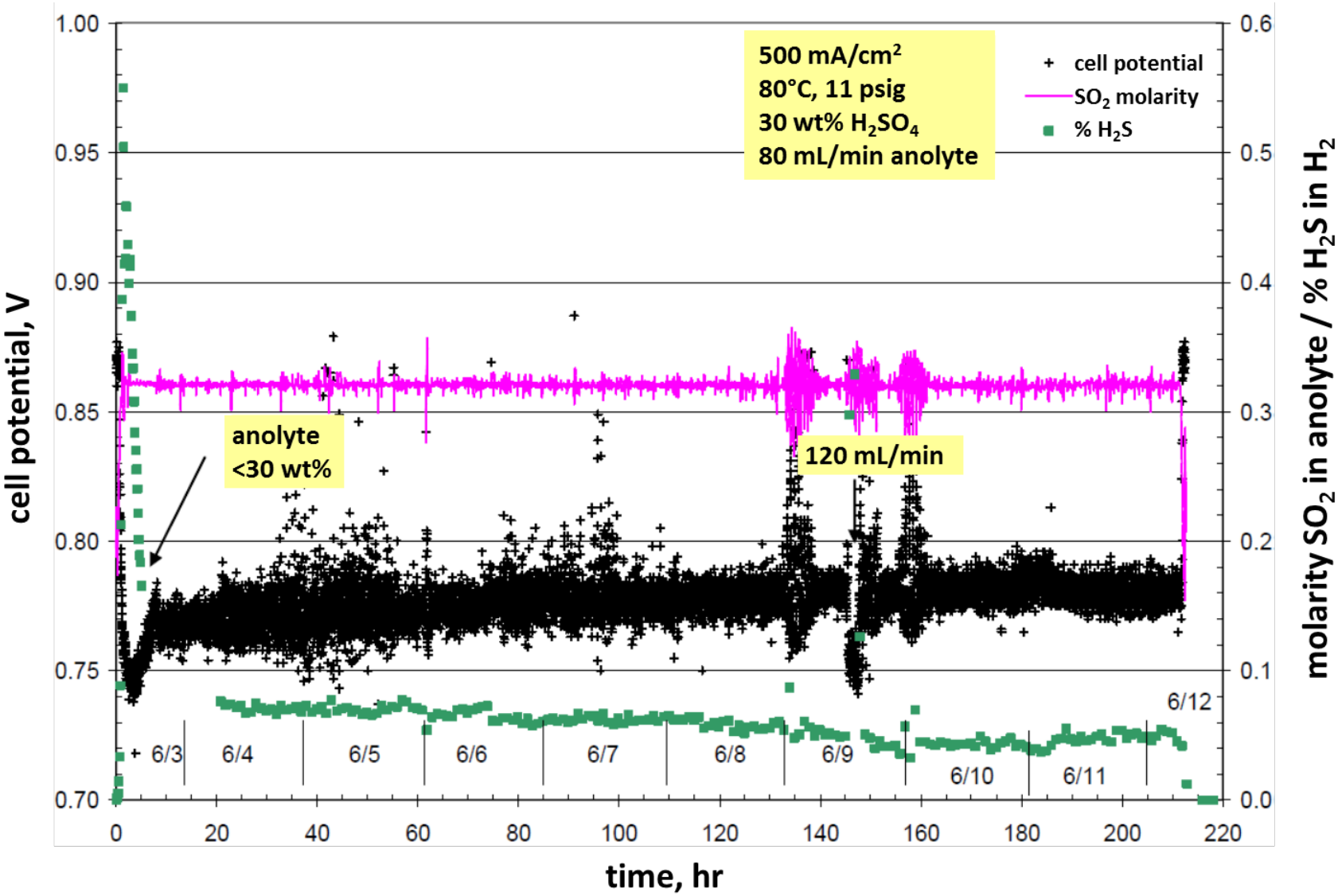
500 mA/cm²
80°C, 11 psig
30 wt% H2SO4
80 mL/min anolyte
cell potential
SO2 molarity
% H2S
anolyte
<30 wt%
120 mL/min
6/3
6/4
6/5
6/6
6/7
6/8
6/9
6/10
6/11
6/12
cell potential, V
molarity SO2 in anolyte / % H2S in H2
time, hr
1.00
0.95
0.90
0.85
0.80
0.75
0.70
0.6
0.5
0.4
0.3
0.2
0.1
0.0
0
20
40
60
80
100
120
140
160
180
200
220

Figure 10

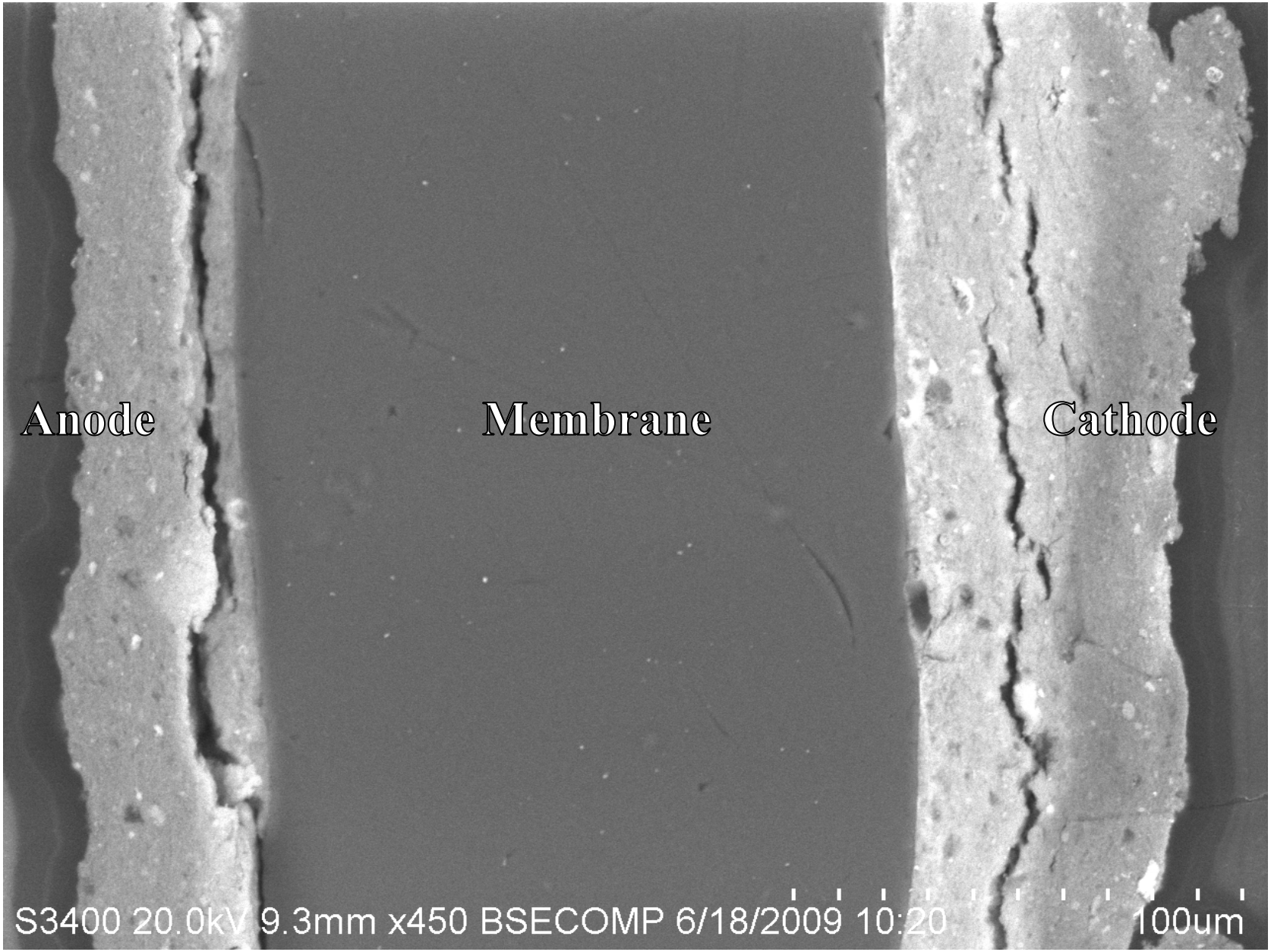
Anode
Membrane
Cathode
S3400 20.0kV 9.3mm x450 BSECOMP 6/18/2009 10:20
100um

Figure 11

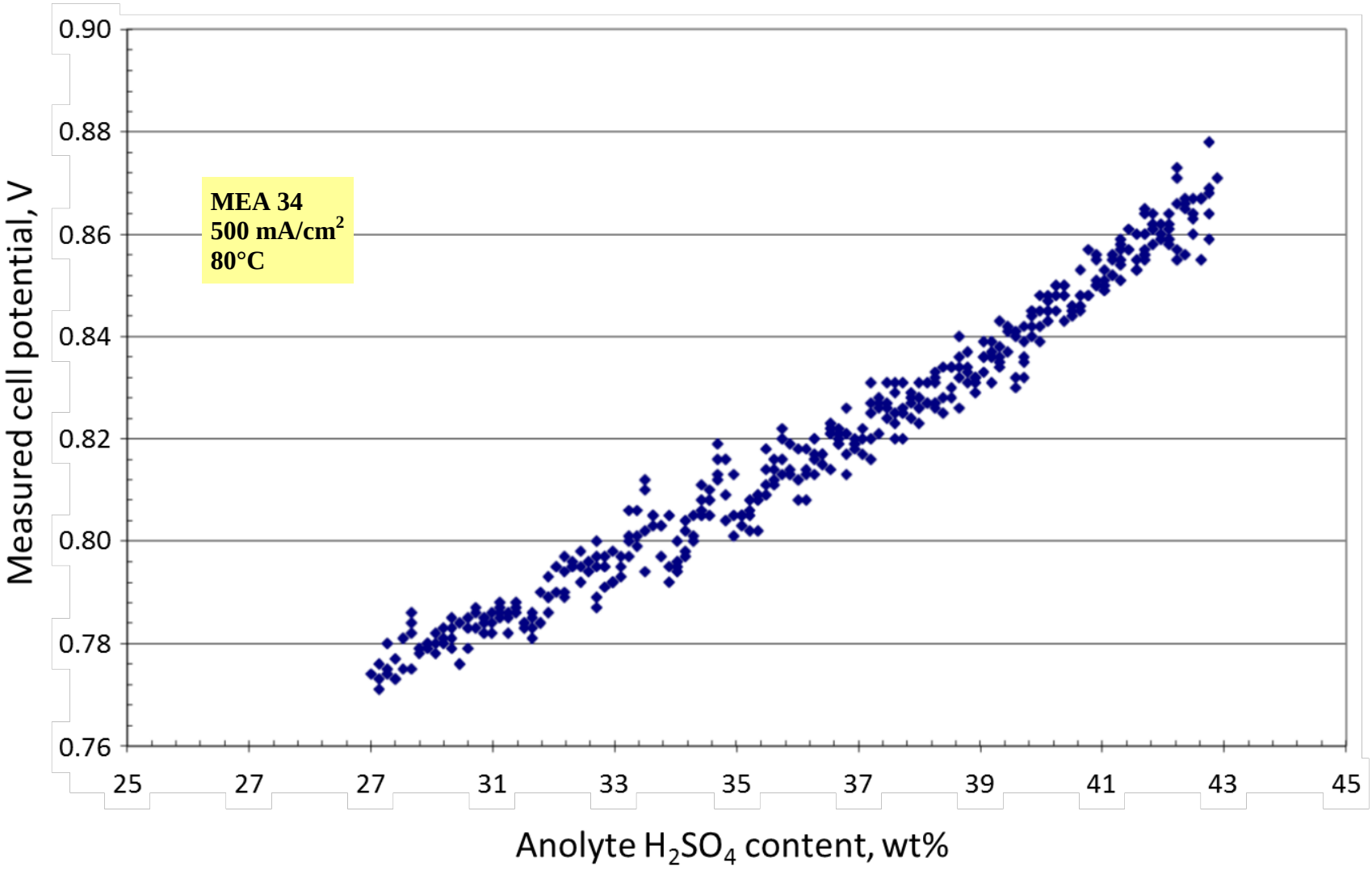
MEA 34
500 mA/cm2
80°C
Measured cell potential, V
0.90
0.88
0.86
0.84
0.82
0.80
0.78
0.76
25
27
27
31
33
35
37
39
41
43
45
Anolyte H2SO4 content, wt%

Figure 12

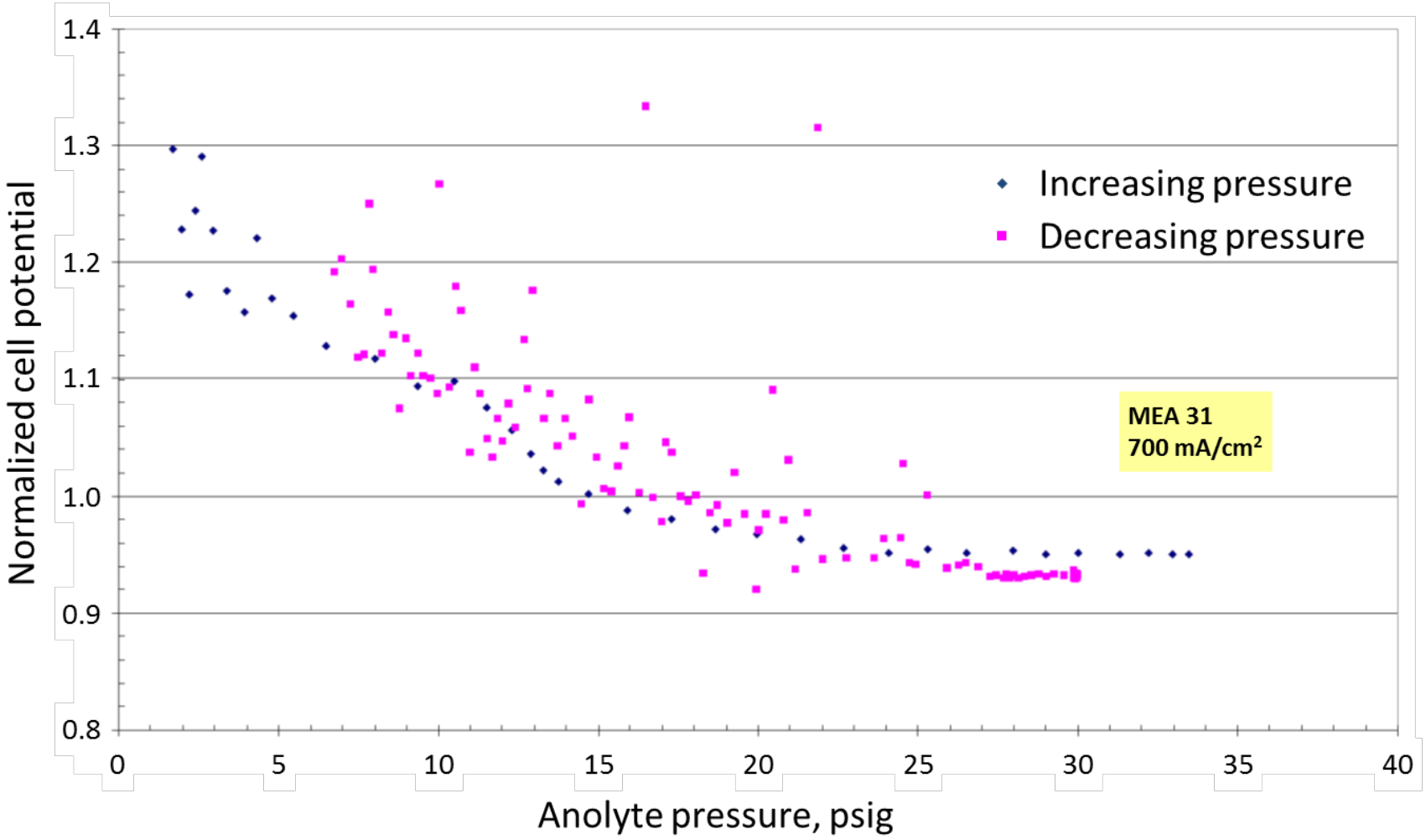
Normalized cell potential
1.4
1.3
1.2
1.1
1.0
0.9
0.8
0
5
10
15
20
25
30
35
40
Anolyte pressure, psig
Increasing pressure
Decreasing pressure
MEA 31
700 mA/cm²

Figure 13

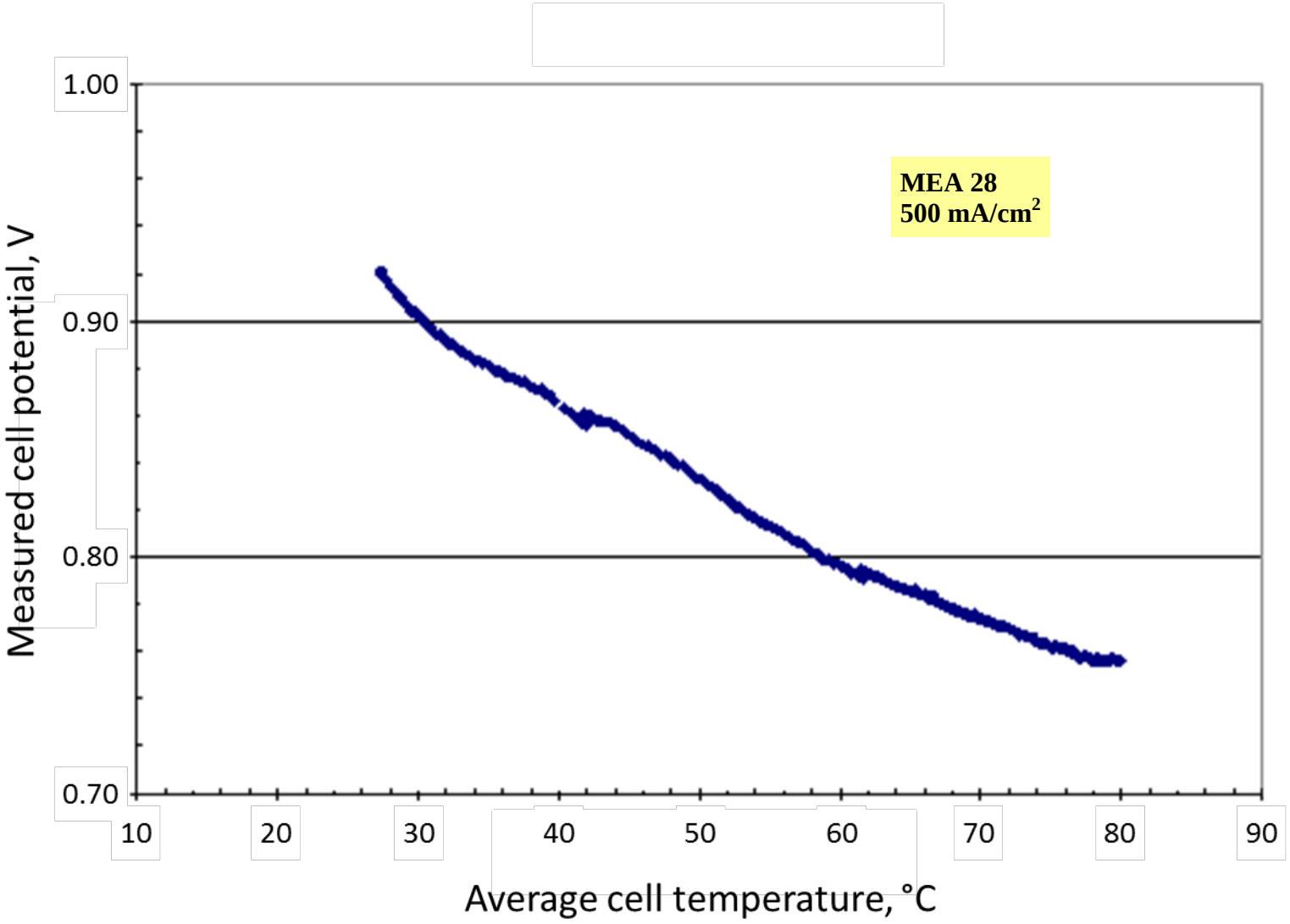
MEA 28
500 mA/cm2
Measured cell potential, V
1.00
0.90
0.80
0.70
10
20
30
40
50
60
70
80
90
Average cell temperature, °C

Figure 14

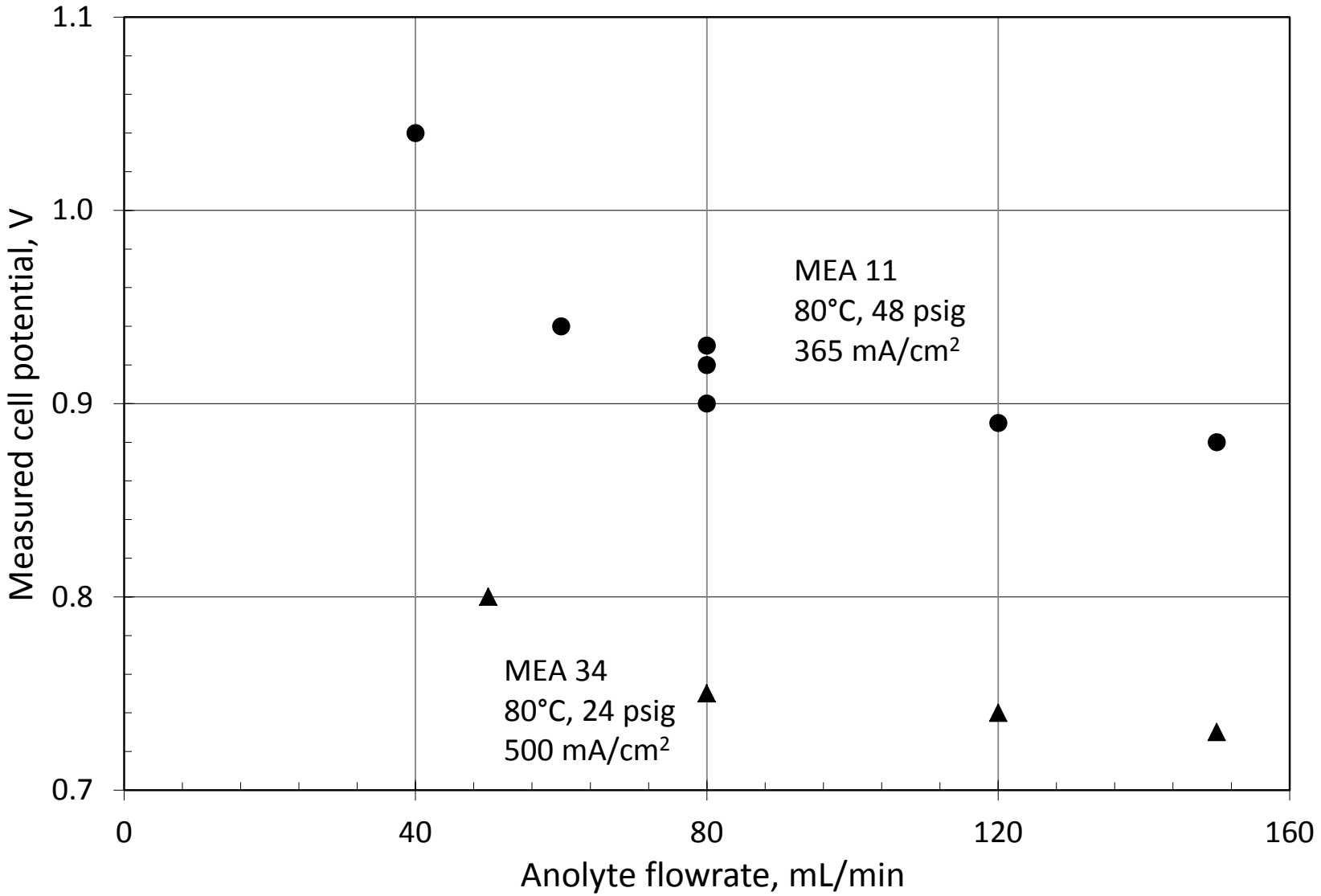
1.1
1.0
0.9
0.8
0.7
Measured cell potential, V
0
40
80
120
160
Anolyte flowrate, mL/min
MEA 11
80°C, 48 psig
365 mA/cm2
MEA 34
80°C, 24 psig
500 mA/cm2

Figure 15

Table 1

MEA No.	Membrane	Membrane thickness, mil	Anode flow field	Cathode flow field	Anode Pt loading, mg/cm^2	Cathode Pt loading, mg/cm^2	Active area, cm^2
1	Nafion® 115	5	E-Tek	E-Tek	0.65 Pt-C	0.65 Pt-C	49.0
2	Nafion® 117	7	Carbon paper, 7 mil	Carbon cloth, 12 mil	1.13 Pt-C	1.14 Pt-C	49.7
3	Nafion® 117	7	Carbon paper, 7 mil	Carbon cloth, 12 mil	1.44 Pt-C	1.32 Pt-C	48.1
4	Nafion® 117	7	Carbon paper, 7 mil	Carbon cloth, 12 mil	0.88 Pt-C	0.99 Pt-C	49.7
5	Celtec®-L	4	Carbon paper, 7 mil	Carbon cloth, 12 mil	1.0 Pt-C	1.0 Pt-C	46.3
6	Celtec®-L (2 layers)	8	Carbon paper, 7 mil	Carbon cloth, 12 mil	1.47 Pt-C	2.16 Pt-C	49.7
7	Celtec®-V	4	Carbon paper, 7 mil	Carbon cloth, 12 mil	0.8 Pt-C	0.8 Pt-C	47
8	Nafion® 115	5	Carbon paper, 7 mil	Carbon cloth, 12 mil	0.78 Pt-C	0.61 Pt-C	49.7

MEA No.	Membrane	Membrane thickness, mil	Anode flow field	Cathode flow field	Anode Pt loading, mg/cm^2	Cathode Pt loading, mg/cm^2	Active area, cm^2
9	Nafion® 117 Giner	7	Carbon paper, 7 mil	Carbon cloth, 12 mil	4.0 Pt black	4.0 Pt black	49.7
10	Nafion® 117 Giner	7	Carbon paper, 7 mil	Carbon cloth, 12 mil	1.0 Pt-C	1.0 Pt-C	49.7
11	Nafion® 115	5	Carbon paper, 7 mil	Carbon cloth, 12 mil	1.09 Pt-C	0.72 Pt-C	47.6 and 54.8
12	Nafion® 115	5	Carbon paper, 7 mil	Carbon cloth, 12 mil	1.01 Pt-C	1.01 Pt-C	54.8
13	Nafion® 115	5	Carbon paper, 7 mil	Carbon cloth, 12 mil	1.02 Pt-C	0.59 Pt-C	54.8
14	Nafion® 117 Giner	7	Carbon paper, 7 mil	Carbon cloth, 12 mil	0.8 Pt-C	0.8 Pt-C	49
15	Polyphenylene SDAPP 2.2 (Hickner)	2	Carbon paper, 7 mil	Carbon cloth, 12 mil	1.5 Pt black	1.5 Pt black	46.3
16	Polyphenylene SDAPP 2.2 (Hickner)	2	Carbon paper, 7 mil	Carbon cloth, 12 mil	1.5 Pt-C	1.5 Pt-C	54.8
17	Nafion® 212 Lynntech	2	Carbon paper, 7 mil	Carbon cloth, 12 mil	1.5 Pt black	1.5 Pt black	50.0

MEA No.	Membrane	Membrane thickness, mil	Anode flow field	Cathode flow field	Anode Pt loading, mg/cm^2	Cathode Pt loading, mg/cm^2	Active area, cm^2
18	Nafion® 115	5	Carbon paper, 7 mil	Carbon cloth, 12 mil	0.75 Pt-C	0.75 Pt-C	54.8
19	Nafion® 115	5	Carbon paper, 7 mil	Carbon cloth, 12 mil	0.83 Pt-C	0.7 Pt-C	54.8
20	Nafion® 115	5	Carbon paper, 7 mil	Carbon cloth, 12 mil	0.782 Pt-C	2.67 Pt black	54.8
21	Nafion® 115	5	Carbon paper, 7 mil	Carbon cloth, 12 mil	0.6 Pt-C	2.9 Pt black	54.8
22	Nafion® 117 Pt impregnated Giner	7	Carbon paper, 7 mil	Carbon cloth, 12 mil	1.0 Pt black	1.0 Pt black	54.8
23	Nafion® 117 Pt impregnated Giner	7	Carbon paper, 7 mil	Carbon cloth, 12 mil	1.0 Pt-C	1.0 Pt black	54.8
24	Nafion® 117 Pt impregnated Giner	7	Carbon paper, 7 mil	Carbon cloth, 12 mil	1.0 Pt-C	1.0 Pt black	48.8
25	Nafion® 117 Giner	7	Carbon paper, 7 mil	Carbon cloth, 12 mil	4.0 Pt black	4.0 Pt black	54.8
26	Nafion® 117 Giner	7	Carbon paper, 7 mil	Carbon cloth, 12 mil	4.0 Pt black	4.0 Pt black	54.8

MEA No.	Membrane	Membrane thickness, mil	Anode flow field	Cathode flow field	Anode Pt loading, mg/cm^2	Cathode Pt loading, mg/cm^2	Active area, cm^2
27	Nafion® 115	5	Carbon paper, 7 mil	Carbon cloth, 12 mil	0.86 Pt-C	1.8 Pt-C	54.8
28	Nafion® 115	5	Carbon paper, 7 mil	Carbon cloth, 12 mil	1.79 Pt-C	0.87 Pt-C	54.8
29	Nafion® 115	5	Carbon paper, 7 mil	Carbon cloth, 12 mil	1.79 Pt-C	0.88 Pt-C	50.0
30	Nafion® 115	5	Carbon paper, 7 mil	Carbon cloth, 12 mil	0.86 Pt-C	1.80 Pt-C	54.8
31	Nafion® 115	5	Carbon paper, 7 mil	Carbon cloth, 12 mil	0.95 Pt-C	1.76 Pt-C	54.8
32	Nafion® 115	5	Carbon paper, 7 mil	Carbon cloth, 12 mil	1.77 Pt-C	0.84 Pt-C	54.8
33	Nafion® 115	5	Carbon paper, 7 mil	Carbon cloth, 12 mil	1.92 Pt-C	0.81 Pt-C	54.8
34	Nafion® 115	5	Carbon paper, 7 mil	Carbon cloth, 12 mil	0.82 Pt-C	1.87 Pt-C	54.8
35	Nafion® 115	5	Carbon paper, 7 mil	Carbon cloth, 12 mil	0.92 Pt-C	1.85 Pt-C	54.8

MEA No.	Membrane	Membrane thickness, mil	Anode flow field	Cathode flow field	Anode Pt loading, mg/cm^2	Cathode Pt loading, mg/cm^2	Active area, cm^2
36	Nafion® 115	5	Carbon paper, 7 mil	Carbon cloth, 12 mil	0.85 Pt-C	1.84 Pt-C	54.8
37	Nafion® 115	5	Carbon paper, 7 mil	Carbon cloth, 12 mil	1.81 Pt-C	0.87 Pt-C	54.8

Development and testing of a PEM SO_2-depolarized electrolyzer and an operating method that prevents sulfur accumulation

Highlights

- A PEM SO_2-depolarized electrolyzer was built and tested for the hybrid sulfur cycle
- 37 different membrane electrode assemblies were tested
- Sulfur deposition was observed at the cathode in early testing
- The sulfur formation mechanism was identified and preventive measures developed
- Operation without sulfur deposition for over 200 h was successfully demonstrated